HYDRODYNAMIC ANALYSIS OF THE NOVEL 360 AIR-LOOP SERIES BIOREACTOR (360-ASBR) FOR MICROALGAE PRODUCTION

By

Hailey Schleining

A Thesis Submitted to the Faculty of the

DEPARTMENT OF BIOSYSTEMS ENGINEERING

In Partial Fulfillment of the Requirements

For the Degree of

MASTER OF SCIENCE

In the Graduate College

THE UNIVERSITY OF ARIZONA

2024

THE UNIVERSITY OF ARIZONA
GRADUATE COLLEGE

As members of the Master's Committee, we certify that we have read the thesis prepared by: Hailey Schleining

titled: Hydrodynamic Analysis of the 360 Air-Loop Series Bioreactor (360-ASBR) for Microalgae Production

and recommend that it be accepted as fulfilling the thesis requirement for the Master's Degree.

Joel Cuello (May 8, 2024 07:57 PDT)

Joel Cuello — Date: May 8, 2024

Peter Waller — Date: May 8, 2024

Kevin Fitzsimmons — Date: May 8, 2024

Final approval and acceptance of this thesis is contingent upon the candidate's submission of the final copies of the thesis to the Graduate College.

I hereby certify that I have read this thesis prepared under my direction and recommend that it be accepted as fulfilling the Master's requirement.

Joel Cuello (May 8, 2024 07:57 PDT)

Date: May 8, 2024

Joel Cuello
Major Advisor and Thesis Committee Chair
Department of Biosystems Engineering

ACKNOWLEDGMENTS

I'd like to acknowledge my Committee Chair, Dr. Joel Cuello, and my Committee Members, Dr. Peter Waller and Dr. Kevin Fitzsimmons, for their invaluable guidance and expert advice throughout this research project. Additionally, I'd like to thank the Laboratory Assistant in the Biosystems Engineering Lab, Dr. Matthew Katterman, whose assistance played a crucial role during the experimental phases of this project. I would also like to extend my appreciation to the entire BE Department for their continuous support and encouragement. Lastly, I want to express my heartfelt gratitude to my family for talking through my research with me.

TABLE OF CONTENTS

LIST OF FIGURES AND TABLES

ABSTRACT

Microalgae are vital microorganisms due to their role in oxygen production, marine ecosystems, and as a source of various high-value products such as vitamins, biofuel, livestock feed, cosmetics, and more. Within some applications, challenges arise in large-scale microalgae production, characterized by high costs and growth rates that fall short of meeting commercial production demands. Therefore, there is still a need for further research to be conducted on microalgae strains and cultivation systems to improve costs and production rates. The focus of this study was to research a novel, patent-pending 360 Air-Loop Series Bioreactor (360-ASBR) and compare it to a Bubble Column Bioreactor (BCBR) that serves as the control. The specific objectives were to (1) determine and compare the hydrodynamic variables of the 360-ASBR and the BCBR including mixing time, residence time, and oxygen liquid mass transfer coefficient (K_La) and (2) determine the effect of the amount and placement of spargers in the BCBR. The results of this study showed that: (1) the mixing time of 198 seconds for the high flow rate and 247 seconds for the low flow rate for the ASBR significantly exceeded that of 25.1 seconds and 38.7 seconds respectively for the BCBR (2) the average residence time of 829 seconds was not significantly less than 1048 seconds for the BCBR at the high flow rate whereas the average residence time of 698 seconds for the ASBR was significantly less than 1053 seconds for the BCBR at the low flow rate, (3) the K_La of 0.012 s^{-1} for the ASBR was not significantly higher than 0.011 s^{-1} for the BCBR at the high flow rate whereas 0.009 s^{-1} for the ASBR significantly exceeded the K_La of 0.002 s^{-1} for the BCBR at the low flow rate, and (4) the mixing times of 25.1, 25.0, and 29.5 s for each sparger arrangement at the high flow rate and 38.7, 29.8, and 39.2 s for each sparger arrangement at the low flow rate did not result in significant differences. The principal conclusions drawn from the results were as follows: (1) the ASBR and the BCBR had

statistically indistinguishable average residence time and K_La at the high flow rate; (2) the BCBR yielded shorter mixing time than the ASBR at both high and low flow rates; and (3) the placement and amount of spargers did not affect the mixing time results in the BCBR. The longer mixing time for the ASBR could be explained by its defined flow path, serving to constrain its bulk liquid mixing within the relatively narrow confines of such a flow path. On scale-up, such defined flow paths are expected to serve the ASBR well in that it ensures and preserves the integrity of its bulk flow patterns independently of the bioreactor volume. By contrast, the BCBR, lacking such defined flow paths, is known in industry and literature to suffer a significant reduction in its mixing efficiency on scale-up.

CHAPTER 1: INTRODUCTION

1.1 Background

1.1.1 Microalgae

Microalgae, also known as microscopic algae, are single-celled eukaryotic microorganisms that are typically found in aquatic environments. Although cyanobacteria, typically included within the microalgae group, are prokaryotic. There are over 30,000 microalgae species that have been scientifically described and it is expected that there are many more species (Thoré et al., 2023). Algae is estimated to have originated over 1 billion years ago, making it one of the oldest life forms thus explaining how they have developed a unique phylogenetic and metabolic diversity (Thoré et al., 2023). Algae's origination is believed to represent the moment oxygen production began in our atmosphere thus initiating the evolution of eukaryotes (Chapman, 2010). Algae remain of high importance to our atmosphere as they produce around half of Earth's total oxygen (Chapman, 2010). Not only are algae important in terms of converting carbon dioxide to oxygen, but they are also essential to marine ecosystems, to the production of high-value compounds, and as a sustainable alternative to multiple products.

Microalgae are rich in nutrients, protein, lipids, and carbohydrates and produce high-value compounds such as carotenoids, polyunsaturated fatty acids, and phycobiliproteins (Garrido-Cardenas et al., 2018). Due to these properties, algae applications vary from nutraceuticals, pharmaceuticals, and cosmetics to biofuels, biofertilizers, livestock feed, and more (Borowitzka, 2013). Additionally, research is being conducted on the use of microalgae for bioremediation processes for wastewater, soils, and flue gases (Garrido-Cardenas et al., 2018). Although microalgae production can be applied to numerous industries, the majority of the algae market, specifically 72%, is attributed to its use in nutritional supplements, pharmaceuticals, and functional food applications (Borowitzka, 2013).

Microalgae has the potential to replace commercial products as a sustainable alternative due to their ability to grow efficiently with minimal nutrient inputs allowing them to achieve higher areal biomass productivity when compared to traditional agriculture crops (Thoré et al., 2023). Additionally, microalgae biomass can be used in full whereas typically only a portion of a traditional crop is utilized (Thoré et al., 2023). Although there are environmental benefits to microalgae production, it can be costly and at times energy-intensive to harvest and process. For example, the production of microalgae biofuels has been researched since the early 2000s although, as of 2023, large-scale production of microalgae does not yet compete with commercial fuel production rates and costs (Thoré et al., 2023). To address these challenges, further research is needed to optimize the microalgae production process.

1.1.2 Algae Cultivation Systems

Microalgae cultivation is reliant on many different factors and environmental conditions including temperature, light, nutrient availability, pH, mixing conditions, hydrodynamic stress, etc. (Zuccaro et al., 2019). Microalgae can be cultured by using an open or closed cultivation system and can use various metabolic pathways including autotrophic, heterotrophic, or mixotrophic (Zuccaro et al., 2019). Open cultivation systems, commonly referred to as open ponds, are exposed to the natural environment and thus utilize free natural resources such as sunlight. These systems have three main classifications: unstirred, raceway, and paddlewheel (Zuccaro et al., 2019). While open ponds have a low initial investment due to their utilization of the environment, they face the challenge of contamination and uncontrolled changes caused by evaporation and the environment. Despite this, open pond systems produce over 80% of algal biomass worldwide (Zuccaro et al., 2019). However, closed photobioreactors (PBRs) are projected to increase in demand and sales due to their advantages over open pond cultivation systems (Zuccaro et al., 2019).

Closed PBRs are vessels or tanks that are illuminated to produce photosynthetic microorganisms, such as microalgae and cyanobacteria. These systems are designed to allow for more control and minimize problems related to contamination, however, do these benefits against open systems, they have additional costs associated with them (Leong et al., 2023). To ensure success, basic criteria for closed systems such as light, circulation, mass transfer, materials, and temperature must be considered (Leong et al., 2023). There are many diverse types of PBRs which are categorized based on their appearance, aeration method, performance, and other factors (Leong et al., 2023). The three main PBR configurations are vertical columns, horizontal tubes, and flat plates.

The design of vertical column PBRs offers several advantages such as being compact, low-cost, having efficient mass transfer, easy to sterilize, and having reduced photo-inhibition (Leong et al., 2023). However, their drawbacks involve the height-to-volume ratio which can create complications at large-scale production if the microalgae strain chosen for the system has high illumination demands (Leong et al., 2023). Within vertical column PBRs, there are bubble column PBRs (BC-PBR), airlift PBRs (A-PBR), and stirred-tank PBRs (ST-PBR).

Bubble Column PBRs (BC-PBRs) are vertical column PBRs in which they are defined by their height being at least twice the diameter or width (Leong et al., 2023). Mixing in BC-PBRs is driven by a sparger located at the bottom of the tank. The design of these bioreactors is simple as shown in Figure 1 and allows for a low investment cost. Additionally, they are known to provide a consistently uniform cultivation environment, along with effective heat and mass transfer and efficient oxygen degassing (Leong et al., 2023). Productivity is highly reliant on the gas flow rate which is the main operating parameter that is affecting the hydrodynamic flow pattern and microalgae circulation (Leong et al., 2023).

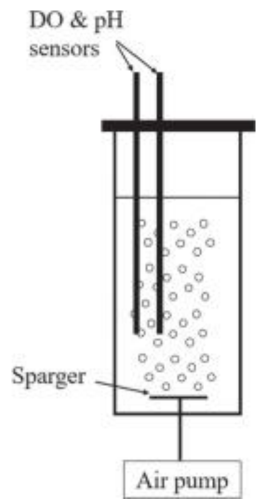

Figure 1. Diagram of bubble column photobioreactor (BC-PBR) (Leong et al., 2023).

Airlift PBRs (A-PBRs) are vertical column PBRs with at least two joined sections (Leong et al., 2023). One of these sections contains an air sparger and is known as the riser due to the bubbles emanating from the sparger driving the liquid upwards (Leong et al., 2023). The other section is known as the downcomer and is the corresponding downward flow of the liquid (Leong et al., 2023). The overall circulation of this BR is caused by a difference in hydrostatic pressure between the riser and downcomer due to the riser being aerated by the sparger (Leong et al., 2023). This flow pattern is said to improve the distribution of bubbles and maximize the mass transfer efficiency (Leong et al., 2023). There are two main configurations of A-PBRs: internal loop and external loop shown in Figure 2. The advantages of this design are simplicity, low energy demand, less shear stress, relatively better performance of gas-liquid mass transfer, and defined cyclic pattern while the disadvantages include cleaning complications and high capital costs (Leong et al., 2023).

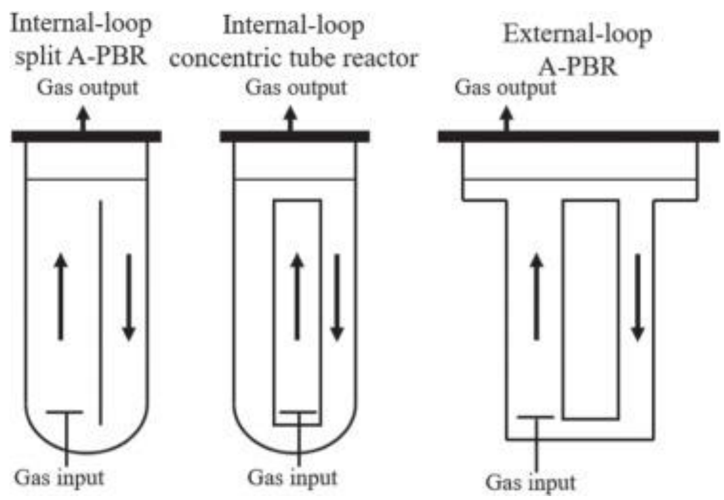

Figure 2. Diagram of airlift photobioreactor (A-PBR) types (Leong et al., 2023).

Stirred-tank PBRs (ST-PBRs) are vertical column PBRs that use mechanical stirring to mix the liquid while a sparger is still used at the bottom to supply air (Leong et al., 2023). This bioreactor allows for the simple installation of sensors shown in Figure 3 but also has some drawbacks. There is a concern with a low surface area to volume ratio causing inefficient light penetration (Leong et al., 2023). While increasing the speed of mechanical stirring can help with this, it will increase undesirable shear stress (Leong et al., 2023). Due to the mechanical stirring component, this design typically requires more energy and generates more heat, thus increasing operational costs.

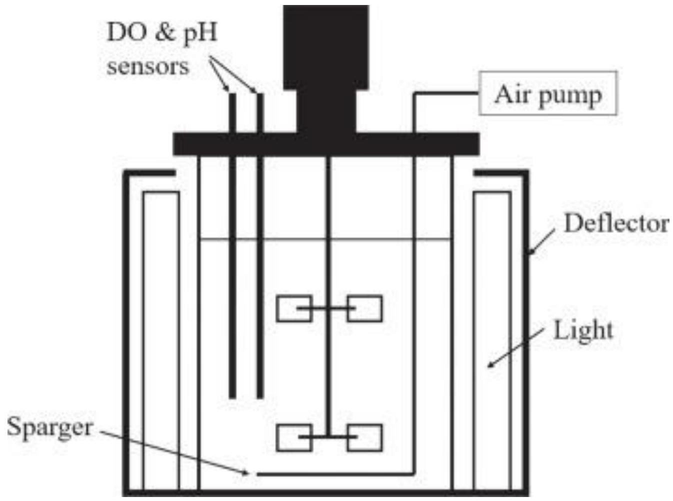

Figure 3. Diagram of stirred-tank photobioreactor (ST-PBR) (Leong et al., 2023).

Horizontal tubular photobioreactors (HT-PBR) can be described as horizontal, parallel tubes with various configurations such as straight (shown in Figure 4), spiral, serpentine looped, manifold type, coiled (helical), and more (Leong et al., 2023). These types of PBRs are regarded as practical and suitable for mass cultivation of microalgae as a result of their large illumination surface area to volume ratio creating a desired light-harvesting efficiency (Leong et al., 2023). If mixing is driven by the use of a pump, the system will likely require high energy input to maintain desired liquid velocities (Leong et al., 2023).

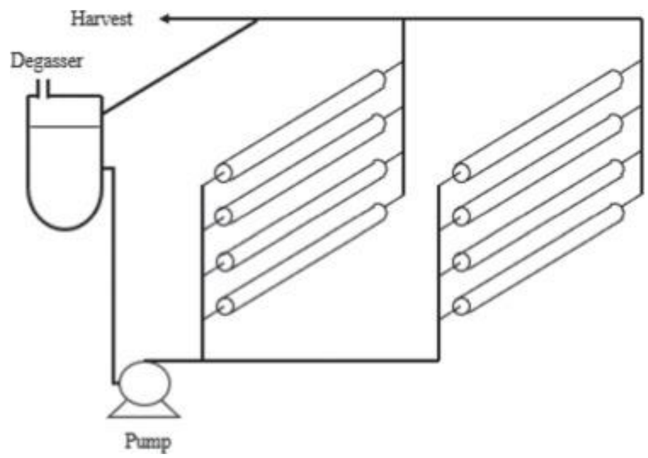

Figure 4. Diagram of horizontal tubular photobioreactor (HT-PBR) (Leong et al., 2023).

Flat plate photobioreactors (FP-PBR) have a simple and compact configuration of a rectangular box with two parallel flat transparent plates placed close together shown in Figure 5 which creates a large illumination surface area to volume ratio and a short light path (Leong et al., 2023). Mixing is achieved through a perforated tube with compressed air located at the bottom and may also be assisted by a mechanical pump if necessary (Leong et al., 2023). These systems have an increased risk of light oversaturation, a possible increase in energy inputs, and a potential for poor mass transfer rates due to the minimal space between the panels resulting in reduced degassing (Leong et al., 2023).

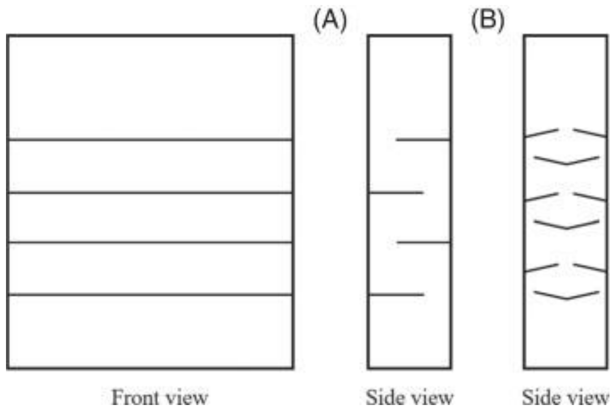

Figure 5. Diagram of flat plate photobioreactors (FP-PBR) with horizontal plates (A) and angled plates (B) (Leong et al., 2023).

There are many other photobioreactors and variations of these main three types. Some include Taylor vortus (TV-PBRs), torus (T-PBRs), and internally illuminated (II-PBRs) (Leong et al., 2023). Most importantly, for commercial applications, a photobioreactor should ideally have a high illumination surface area to volume ratio, high mixing efficiency and mass transfer rate, low energy requirements, smooth control of operating parameters (pH, temperature, dissolved CO2, and O2 concentration), and be able to achieve high biomass productivities with low space requirements (Leong et al., 2023). Determining which configuration to use can depend on the type of microalgae strain, desired product, production cost, desired investment cost, and geographical location (Leong et al., 2023).

1.1.3 Photobioreactor Hydrodynamics

Many factors affect the cultivation of microalgae in photobioreactors, although closed systems allow for the cultivation to be more controlled and thus typically result in higher biomass production. Hydrodynamics, otherwise known as mixing conditions, are a function of the PBR's design and operating setpoints (Babcock et al., 2002). Hydrodynamics greatly affects the light distribution due to the movement of the algae which in turn affects the photosynthetic efficiency, productivity, and cell composition of the culture (Babcock et al., 2002). The goals of PBRs involve effective and efficient provision of light, supply of carbon dioxide with minimal losses, removal of photosynthetically produced oxygen, and effective control of temperature (Babcock et al., 2002). Determining the hydrodynamic condition for each PBR design is essential as the impact on productivity differs depending on the type of system being investigated. Therefore, this study focuses on determining the hydrodynamic condition for the novel 360-ASBR design. The three main variables involved in the classification of the hydrodynamic condition are mixing time, residence time, and oxygen liquid mass transfer coefficient. Achieving optimal mixing is critical to the light distribution and thus overall productivity of the PBR (Babcock et al., 2002). Excessive mixing can be damaging to the algal cells due to increased shear stress and must be considered (Babcock et al., 2002). The volumetric gas-liquid mass transfer coefficient K_La is important in ensuring that oxygen is removed to avoid inhibiting concentrations and that carbon dioxide is transported to support cell growth through photosynthesis (Babcock et al., 2002).

1.2 Objectives and Hypothesis

The objectives of this study were to (1) determine and compare the hydrodynamic variables of the BCBR and the 360-ASBR including mixing time, residence time, and oxygen liquid mass transfer coefficient and (2) determine the effect of the amount and placement of spargers in the BCBR by testing three arrangements. Given the definite internal flow structure of the ASBR, it is expected that it will exhibit overall better hydrodynamic characteristics that will reliably remain stable on scale-up rather than the BCBR. The null hypothesis is that the means of the ASBR and BCBR are equal for each associated experiment and flow rate, whereas the alternative hypothesis is that they are not.

CHAPTER 2: PRESENT STUDY

2.1 Summary

Conducting a hydrodynamic analysis is essential when considering large-scale implementation of a new photobioreactor design. A hydrodynamic analysis of a photobioreactor typically consists of measuring the mixing time, residence time distribution, and oxygen liquid mass transfer coefficient in order to make conclusions regarding the gas and nutrient availability and distribution. The specific objectives of this study were to (1) determine and compare the hydrodynamic variables of the 360-ASBR and the BCBR including mixing time, residence time, and oxygen liquid mass transfer coefficient (K_La) and (2) determine the effect of the amount and placement of spargers in the BCBR. All three hydrodynamic variables were measured 3 times at two different flow rates. The results of this study showed that: (1) the mixing time of 198 seconds for the high flow rate and 247 seconds for the low flow rate for the ASBR significantly exceeded that of 25.1 seconds and 38.7 seconds respectively for the BCBR (2) the average residence time of 829 seconds was not significantly lower than 1048 seconds for the BCBR at the high flow rate whereas the average residence time of 698 seconds for the ASBR was significantly lower than 1053 seconds for the BCBR at the low flow rate, (3) the K_La of 0.012 s^{-1} for the ASBR was not significantly higher than 0.011 s^{-1} for the BCBR at the high flow rate whereas 0.009 s^{-1} for the ASBR significantly exceeded the K_La of 0.002 s^{-1} for the BCBR at the low flow rate, and (4) the mixing times of 25.1, 25.0, and 29.5 s for each sparger arrangement at the high flow rate and 38.7, 29.8, and 39.2 s for each sparger arrangement at the low flow rate did not result in significant differences. The principal conclusions drawn from the results were as follows: (1) the BCBR exhibits greater liquid mixing compared to the ASBR, a desired factor for algal growth rate; (2) the ASBR demonstrates greater mass transfer than the BCBR, also a

desired factor for algal growth rate; and (3) the placement and amount of spargers did not affect our Mixing Time results in the BCBR.

2.2 Methodology and Materials

2.2.1 Experimental Design Overview

Three experiments were conducted, one for each of the hydrodynamic variables under investigation: mixing time, Residence Time Distribution (RTD), and oxygen liquid mass transfer coefficient (K_La). All three experiments have the same four treatments and 3 replicates per treatment. The four treatments, one for each gas flow rate and bioreactor, are the ASBR with a high flow rate, ASBR with a low flow rate, BCBR with a high flow rate, and BCBR with a low flow rate. The high flow rate is set at 13 SCFH (6.14 LPM) and the low flow rate is set at 6.5 SCFH (3.07 LPM) which results in a VVM of 0.1 and 0.05 respectively. VVM is the vessel volume per minute calculated by applying Equation 1.

$$VVM = v/V \tag{1}$$

Where v is the volumetric gas flow rate and V is the aerated volume of the bioreactor. This experimental design is applied to all three experiments. Microalgae growth is not involved in these experiments. R Programming is used for all calculations, graphs, and analyses.

2.2.2 Photobioreactor Design

The experimental bioreactor in this study, the 360 Air-Loop Series Bioreactor (360-ASBR), is representative of an airlift PBR with a novel design. The 360-ASBR is a patent-pending photobioreactor designed and developed in the Biosystems Engineering Laboratory at The University of Arizona. The design utilizes glass inlays as shown in red in Figure 6 along with two spargers shown in blue to create a unique flow pattern that loops around. A sparger typically utilizes a porous stone material that is connected to a gas source in which the gas is introduced to the liquid through bubbles. Subsequently, the 360-ASBR has two risers and two downcomers. The control bioreactor in this study, the Bubble Column Bioreactor (BCBR), is a common vertical column PBR. The BCBR does not have any glass inlays but does have two spargers shown in blue in Figure 6. A photo of the exact bioreactors used in this study is shown in Figure 7.

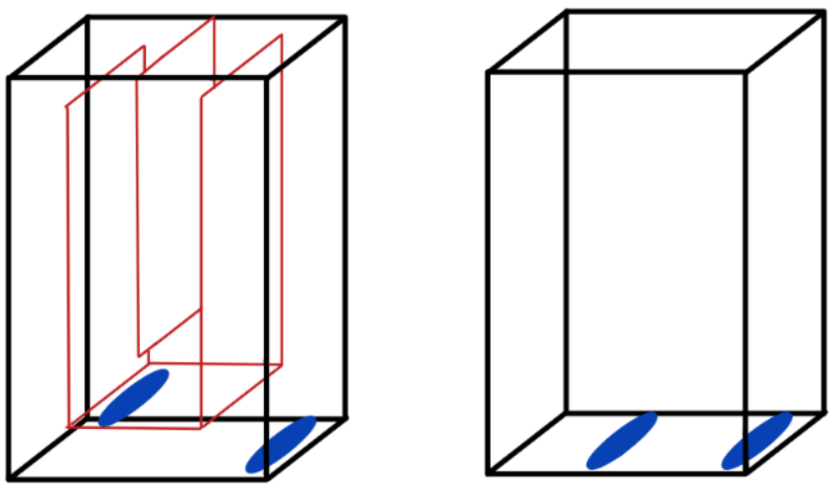

Figure 6. Design of the 360-ASBR (left) and BCBR (right).

Figure 7. Photos of the 360-ASBR (left) and BCBR (right).

2.2.3 Sensors

Two sensors were used in this experiment: a Vernier Conductivity Probe and a Vernier Dissolved Oxygen Probe. Both sensors require calibration as specified in Verniers User Manuals. For the conductivity probe, a three-point calibration was conducted with sodium chloride concentrations in the low, mid, and high ranges as specified by Vernier. The concentrations were 200 µS/cm, 2,000 µS/cm, and 20,000 µS/cm. The concentrations measured with the Conductivity Probe and the known concentrations were utilized to develop a calibration graph. The equation for the line of best fit on this graph is the calibration equation that was applied when recording data with this sensor. A standard linear model was used to calibrate the system using a line of best fit. Then the measured values for the mixing time and RTD experiments were individually input into the calibration equation, to get an adjusted value with an expected accuracy of ±2%.

For the DO probe, a two-point calibration was conducted with the first calibration point being a sodium sulfite calibration solution and the second being deionized water. With the deionized water case, the sensor is held above the water within a secured bottle. This calibration was done by utilizing the Logger Lite Pro Software to input the reading results in which a calibration equation was then applied to all data collection for the K_La experiment.

2.2.4 Mixing Time

Mixing time is defined as the time it takes for a tracer molecule to become evenly distributed within a solution. The tracer molecule used in this study was Sodium Chloride (NaCl). The tracer molecule was measured by using a Vernier Conductivity Probe and applying the associated calibration equation. The experimental design described in Section 2.2.1 was applied to the mixing time experiment. The location of the sensor and NaCl injection point were maintained for all experimental runs and are shown in Figure 8. There were three different sparger placements investigated by measuring the mixing time shown in Figure 9: two spargers placed as shown in Sparger Arrangement 1, one sparger placed as shown in Sparger Arrangement 2, and two spargers placed together as shown in Sparger Arrangement 3. The first placement shown in Figure 8 and Sparger Arrangement 1 represents the standard placement for this study. The other placements allow for the exploration of the effect of sparger placement on the results.

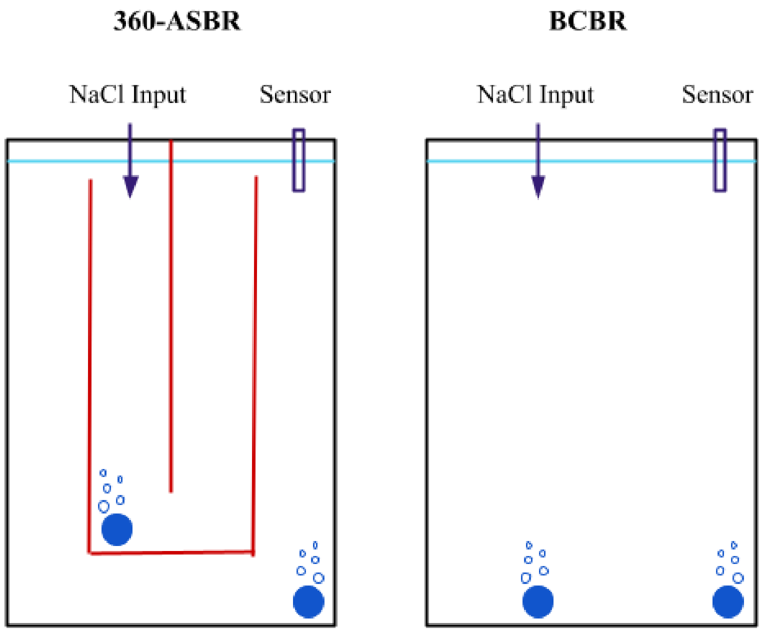

Figure 8. Mixing time experimental setup.

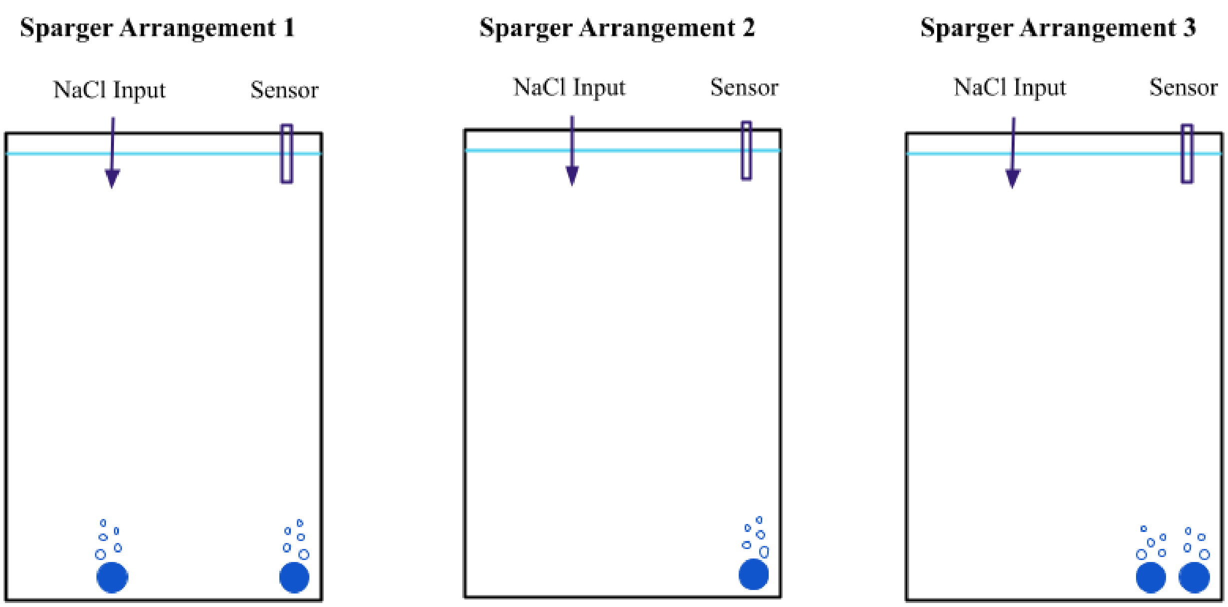

Figure 9. Three sparger arrangements were tested by measuring the mixing time.

Data collected from the sensor was recorded using Logger Lite Computer Software. The mixing time was determined by taking the average of the last 25 values with an added and subtracted 5% to create a range of values. The time at which all values after that point in time remain within the $\pm$5% range represents the mixing time. The results are graphically shown using a line graph. Some graphs had significant noise that disrupted the mixing time determination. To decrease noise, a 3-second moving average was applied to all graphs which allows for an accurate and consistent mixing time determination.

2.2.5 Residence Time Distribution

The residence time is the total time that a molecule has spent in a control volume. The experiment was conducted by using a tracer molecule, Sodium Chloride, and having an input and output that was set at the same flow rate to maintain the volume of the tank. The tracer molecule was measured by using the Vernier Conductivity Probe and the experimental design described in Section 2.2.1 was applied. The data from the sensor was recorded using Logger Lite Computer Software. The location of the deionized water input, output, sensor, and NaCl input were all maintained as shown in Figure 10.

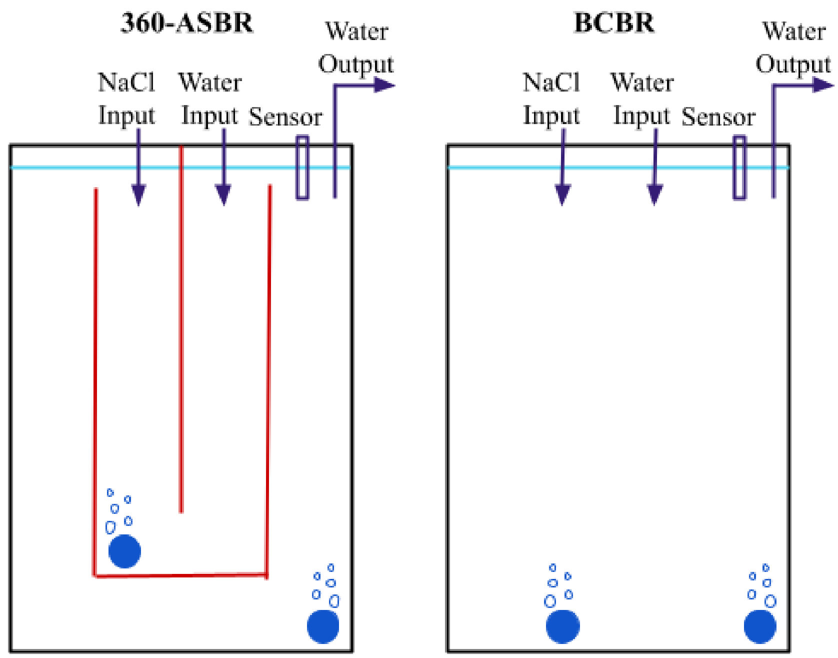

Figure 10. Residence time experimental setup.

The output was gravity fed by a siphon and the water input is adjusted accordingly. Specifically, a 3/8” diameter siphon was used and it is stated by the supplier to have a 0.1 liters per second flow rate. Given the 61.6 L working volume, the system had an approximate exchange time of 616 seconds. The data should start and end at the same concentration, therefore an extrapolation was applied to the collected data using an exponential decay function to approximate how long it takes for the concentration to reach near zero, specifically 0.5 µS/cm. Due to the nature of this function, the majority of the final data points represent small concentration values. With the collected and extrapolated data combined by using a bleed in R, Equation 2 was then applied to determine the average solution residence time.

$$t^* = \frac{\sum t_i C_i \Delta t_i}{\sum C_i \Delta t_i} \tag{2}$$

Where t^* is the average residence time in seconds, t is time, C is concentration, and i is each element in the vector C. The RTD itself, also known as the E curve, is shown graphically by normalizing the original residence time curve. This was achieved by calculating the area in Equation 3 and then applying the result in Equation 4 to generate a graph with an integral of 1.

$$area = \left(\sum_{i=1}^{n-1} combinedC_{i+1} - \ combinedC_i \right) * time_n \tag{3}$$

Where $combinedC$ represents the data that includes the collected data with the extrapolated data, i represents each element in the vector $combinedC$, and n is the number of elements in the vector $combinedC$.

$$RTD_i = \frac{combinedC_i}{area} \tag{4}$$

This equation generates a new vector, RTD, which was graphed against time to result in an area of 1. The Vessel Dispersion number was then calculated in order to characterize the flow behavior and deviation from ideal plug flow within the bioreactors. In ideal plug flow, the velocity gradient and direction of the flow are consistent and smooth whereas in mixed flow, there will be some inconsistency with the velocity and flow direction, such as back mixing. The Vessel Dispersion number is represented by D/uL which is the coefficient of axial dispersion in the dimensionless form of Fick's Law of Dispersion shown in Equation 5.

$$\frac{\partial C}{\partial \theta} = \left(\frac{D}{uL} \right) \frac{\partial^2 C}{\partial z^2} - \ \frac{\partial C}{\partial z} \tag{5}$$

Where C is concentration, θ is the dimensionless time, D is the dispersion coefficient, μ is the average fluid velocity, L is the length of the system, and z is the length from entrance divided by the length of the system. When D/uL -> 0 represents plug flow and D/uL -> ∞ represents mixed flow. The Vessel Dispersion number was calculated by the variance of the RTD data. Lastly, the Bodenstein number was calculated by taking the inverse of the Vessel Dispersion number, thus equaling uL/D.

2.2.6 Oxygen Liquid Mass Transfer Coefficient (K_La)

This experiment was conducted by adding nitrogen gas through the spargers in order to decrease the dissolved oxygen concentration. Once oxygen levels reached a minimum, the nitrogen gas was replaced with air. The rise in oxygen concentration over time was measured using a Vernier Dissolved Oxygen Probe connected to Logger Lite Software. The location of the sensor was maintained as shown in Figure 11.

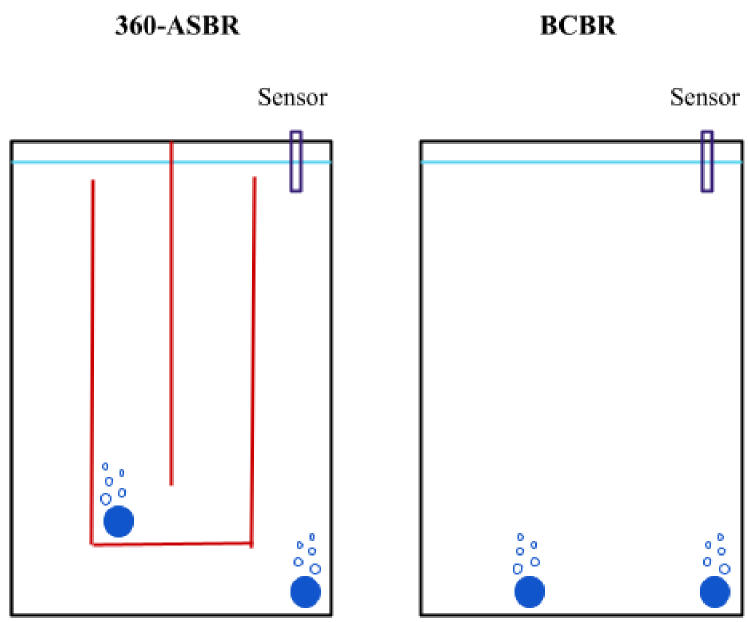

Figure 11. KLa experimental setup.

Once the dissolved oxygen and time data were collected, Equation 6 was applied to calculate K_La.

$$K_La = \ln(\frac{C_s - C_2}{C_s - C_1}) \times \frac{1}{t_1 - t_2} \quad (6)$$

Where C_s is the saturation oxygen concentration and C_1 and C_2 are oxygen concentrations at time t_1 and t_2 respectively. This was graphically determined by creating a new K_La vector by applying a rearrangement of Equation 6 shown in Equation 7.

$$K_La_i = -\ln(\frac{C_s - C_i}{C_s - C_1}) \quad (7)$$

Where i represents each element in the K_La vector and C_1 represents the first value in the vector. This new vector was then plotted against time and a line of best fit was applied. The slope of the line of best fit represents the K_La value.

2.2.7 Statistical Analysis

The means and standard deviations for each treatment group within each experiment were calculated. Then the ASBR results were compared to the BCBR results individually for each flow rate by using a t-test with a significance level of 0.05. Therefore, there is a 5% probability of rejecting or failing to reject the null hypothesis mistakenly. An ANOVA test was conducted to analyze the sparger arrangements for each flow rate. If the p-value is less than 0.05 then the null hypothesis is rejected and there is a statistically significant difference between the PBRs for the variable under investigation. Conversely, if the p-value is above 0.05, then the null hypothesis is not rejected and the alternative hypothesis is true. The R Programming codes for all data and statistical analysis can be found in the Appendix.

2.3 Results and Discussion

2.3.1 Results Overview

Table 1 shows the p-value results for each measured value at each flow rate in which the mean results for the three replicates from the ASBR and BCBR were compared.

Table 1. P-Value results for all values measured.

P-VALUE RESULTS					
	Flow Rate	**P-Value**	**Replicate 3**	**Flow Rate**	**P-Value**
Mixing Time	*High*	0.013	**Bodenstein**	*High*	0.101
	Low	0.001		*Low*	0.102
RTD	*High*	0.197	**K_La**	*High*	0.173
	Low	0.023		*Low*	0.022
Vessel Dispersion	*High*	0.095	**Sparger Arrangement**	*High*	0.200
	Low	0.090		*Low*	0.066

Comparing these values to the significance level of 0.05, it is observed that there was statistical significance for the mixing time at the high and low flow rates and for the residence time and K_La at only the low flow rate.

2.3.2 Mixing Time

The moving average filter was applied as shown for one of the replicates in Figure 12 for the ASBR and Figure 13 for the BCBR. Each replicate for each treatment has an associated graph depicting the ±5% range and the point at which the mixing time lies on the graph.

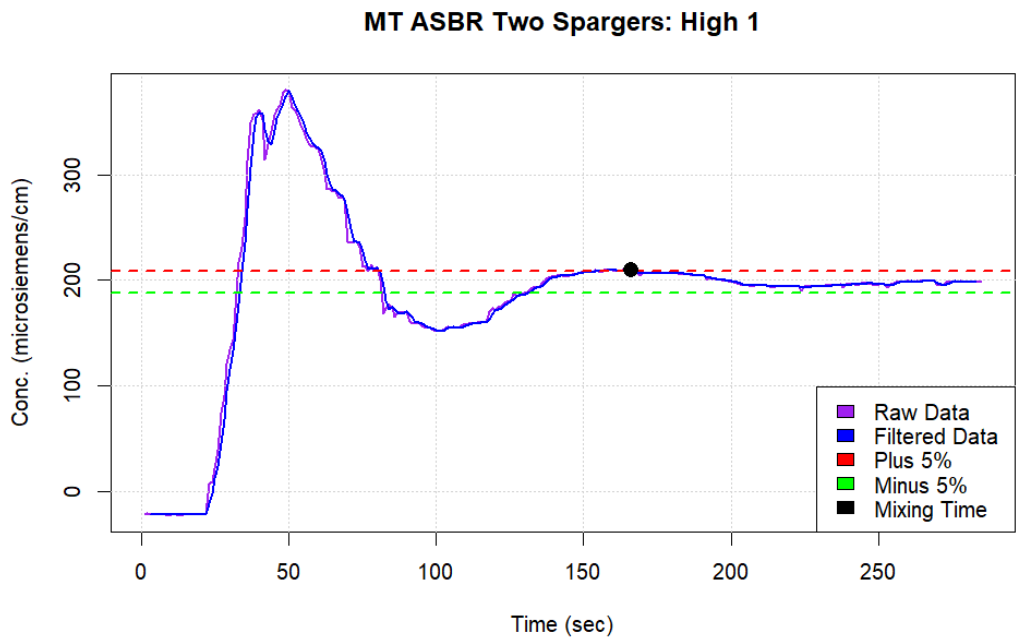

Figure 12. Mixing Time Result for one of the replicates from the ASBR.

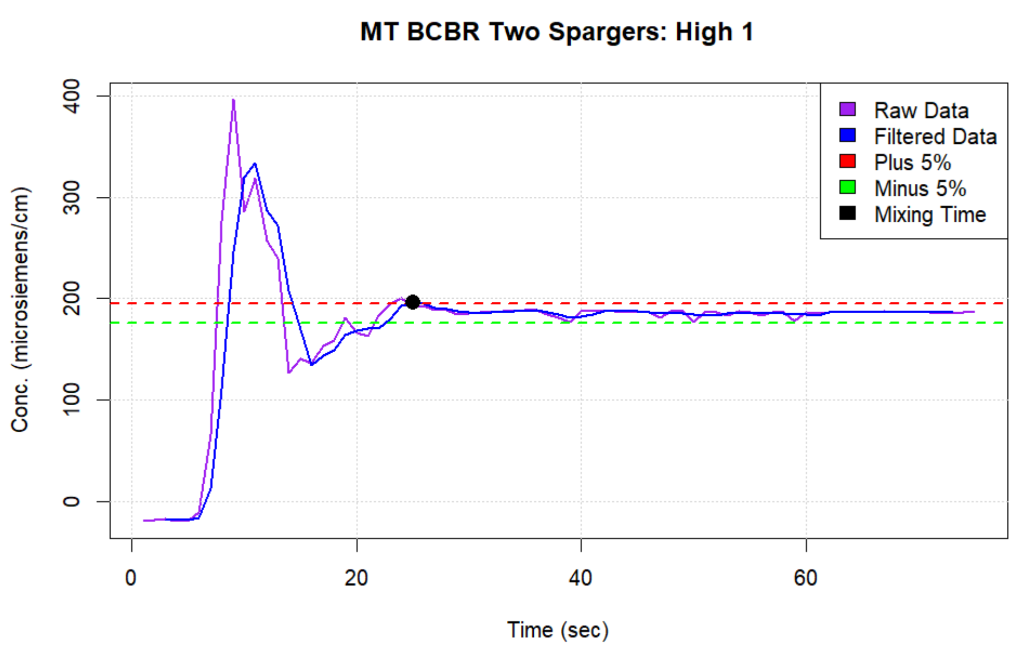

Figure 13. Mixing Time Result for one of the replicates from the ASBR.

The moving average filter was more pronounced for the BCBR results than the ASBR because the concentration peaks at a much more rapid rate. Each replication result is graphically shown in Figures 24 to 27 in the Appendix. Table 2 shows the values for each treatment and replication.

Table 2. Mixing Time results for all treatment groups.

MIXING TIME RESULTS: TWO SPARGERS (Units: seconds)						
	Flow Rate	**Replicate 1**	**Replicate 2**	**Replicate 3**	**Mean**	**Std. Dev.**
ASBR	*High*	166	193	236	198	35.2
	Low	259	235	247	247	12.3
BCBR	*High*	28.9	23.2	23.3	25.1	3.26
	Low	40.6	36.7	38.7	38.7	1.98

The mean mixing time and standard deviation for each treatment group are shown in Figure 14.

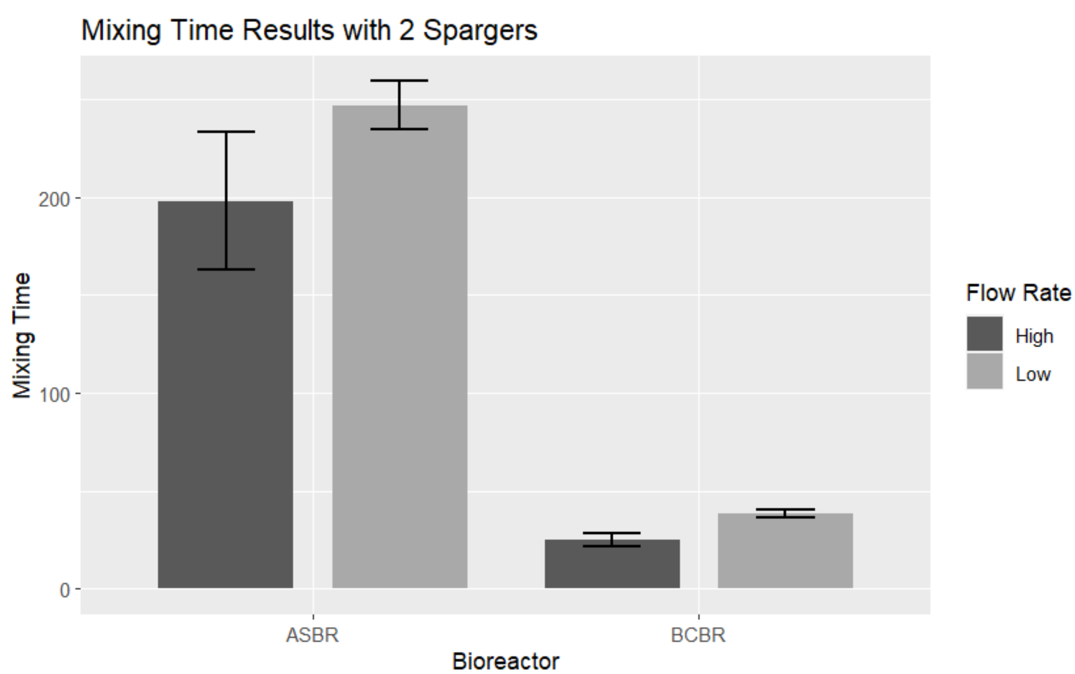

Figure 14. Depicts the mean and standard deviation for each treatment group in the Mixing Time experiment.

The mean mixing time for the high flow rate resulted in a statistically significant difference between the bioreactors with a p-value of 0.013 which is less than our significant level of 0.05.

Additionally, the mean mixing time for the low flow rate showed a stronger statistically significant difference between the bioreactors with a lower p-value of 0.001. There was a prominent difference in the mixing time results between the two bioreactors, with the ASBR having a higher mixing time. This is because the ASBR has a defined flow path whereas the BCBR does not. Therefore, the tracer molecule had a longer path to flow through until it became fully mixed within the ASBR. Generally, a shorter mixing time is desired, however a defined flow path is important for scaling up.

2.3.3 Residence Time Distribution

The exponential decay extrapolation applied to the residence time and the associated normalization with the combined data is shown in Figure 15 for the ASBR and Figure 16 for the BCBR.

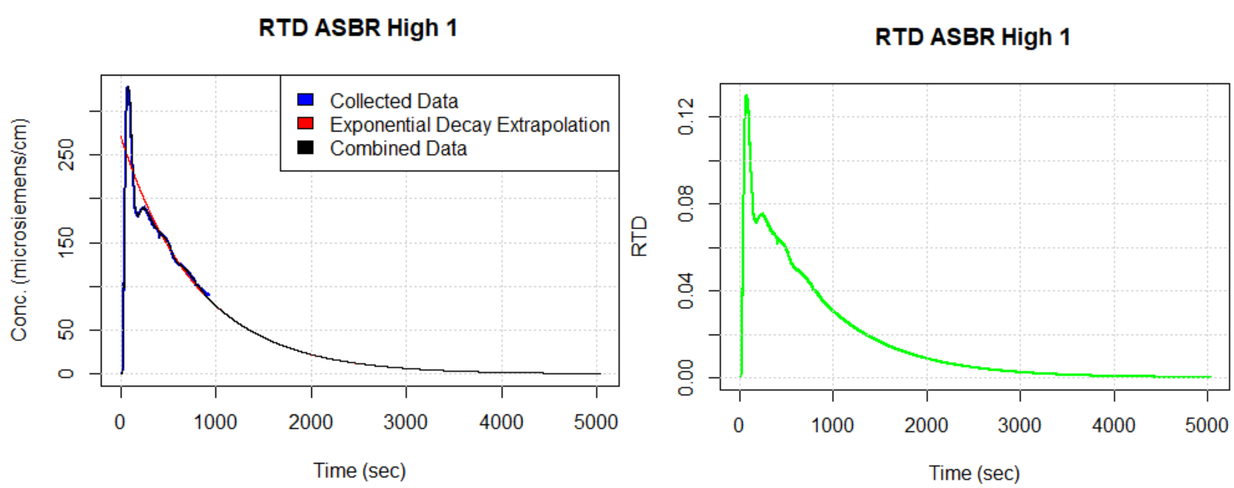

Figure 15. RTD Graphs for one of the replicates for the ASBR.

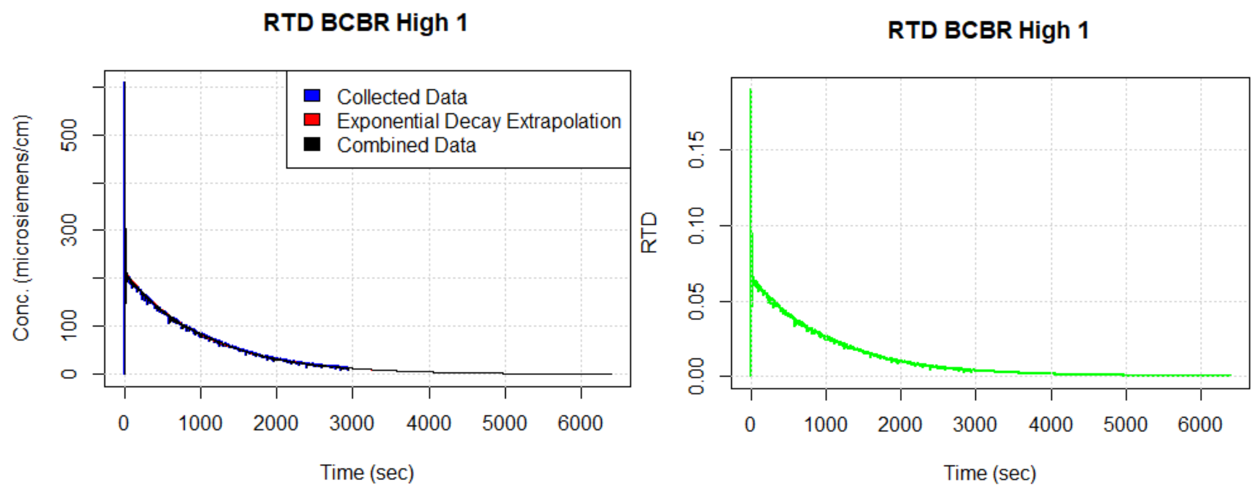

Figure 16. RTD Graphs for one of the replicates for the BCBR.

Each replication result is graphically shown in Figures 32 to 35 in the Appendix. Table 3 shows the values for each treatment and replication.

Table 3. Residence Time Distribution results with the Average Residence Time (RT), Vessel Dispersion Number (D/uL), and Bodenstein number (Bo) for each treatment.

RESIDENCE TIME DISTRIBUTION RESULTS (Units: seconds)							
	Flow Rate	**Value**	**Replicate 1**	**Replicate 2**	**Replicate 3**	**Mean**	**Std. Dev.**
ASBR	*High*	RT	827	630	1028	829	199
		D/uL	0.432	0.424	0.455	0.437	0.016
		Bo	2.32	2.36	2.20	2.29	0.083
	Low	RT	621	807	667	698	96.8
		D/uL	0.398	0.444	0.419	0.420	0.023
		Bo	2.51	2.25	2.39	2.38	0.130
BCBR	*High*	RT	1044	1048	1051	1048	3.62
		D/uL	0.465	0.465	0.463	0.464	0.001
		Bo	2.15	2.15	2.16	2.15	0.005
	Low	RT	1055	1060	1043	1053	8.57
		D/uL	0.464	0.461	0.460	0.462	0.002
		Bo	2.16	2.17	2.17	2.17	0.009

The mean residence time and standard deviation for each treatment group are shown in Figure 17. The mean Vessel Distribution number and standard deviation for each treatment group are shown in Figure 18, and the mean Bodenstein number and standard deviation for each treatment group are shown in Figure 19.

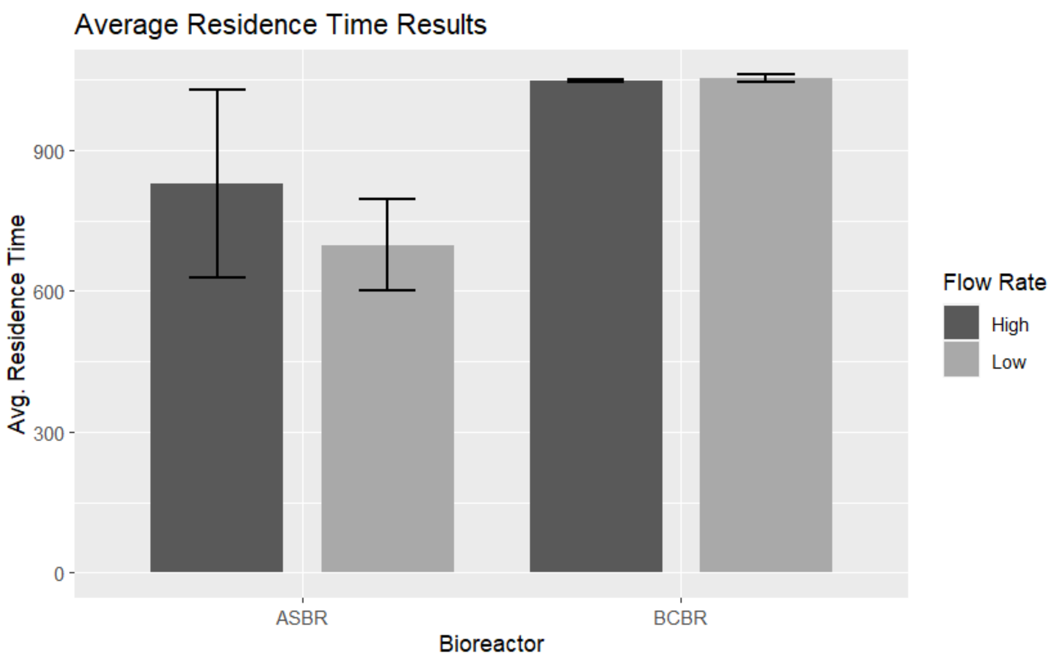

Figure 17. Depicts the mean and standard deviation for each treatment group for the Average Residence Time results.

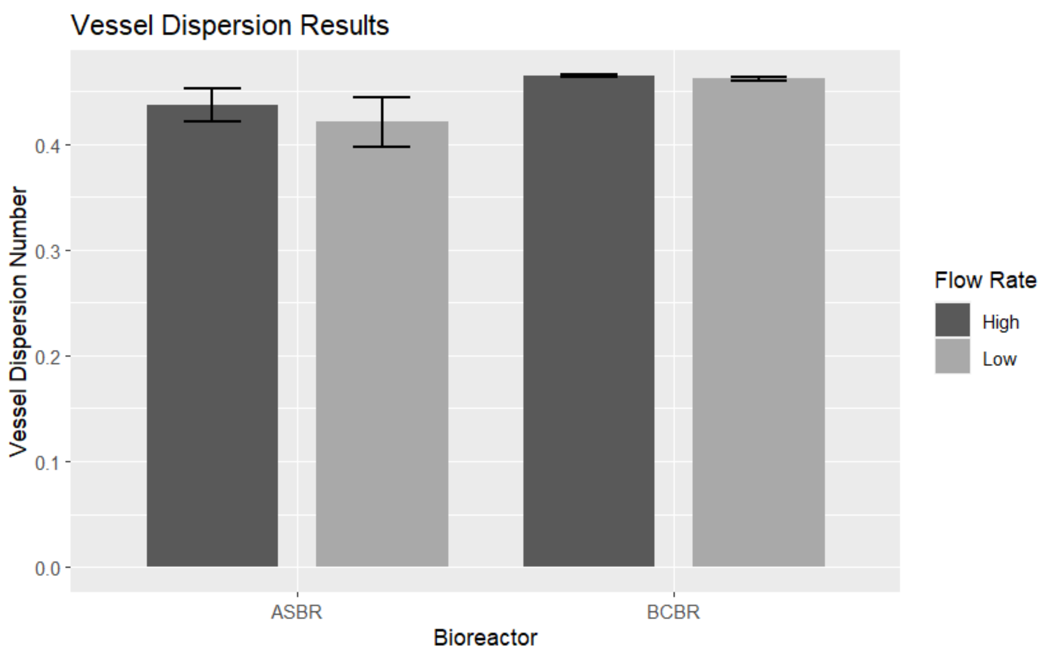

Figure 18. Depicts the mean and standard deviation for each treatment group for the Vessel Dispersion Number results.

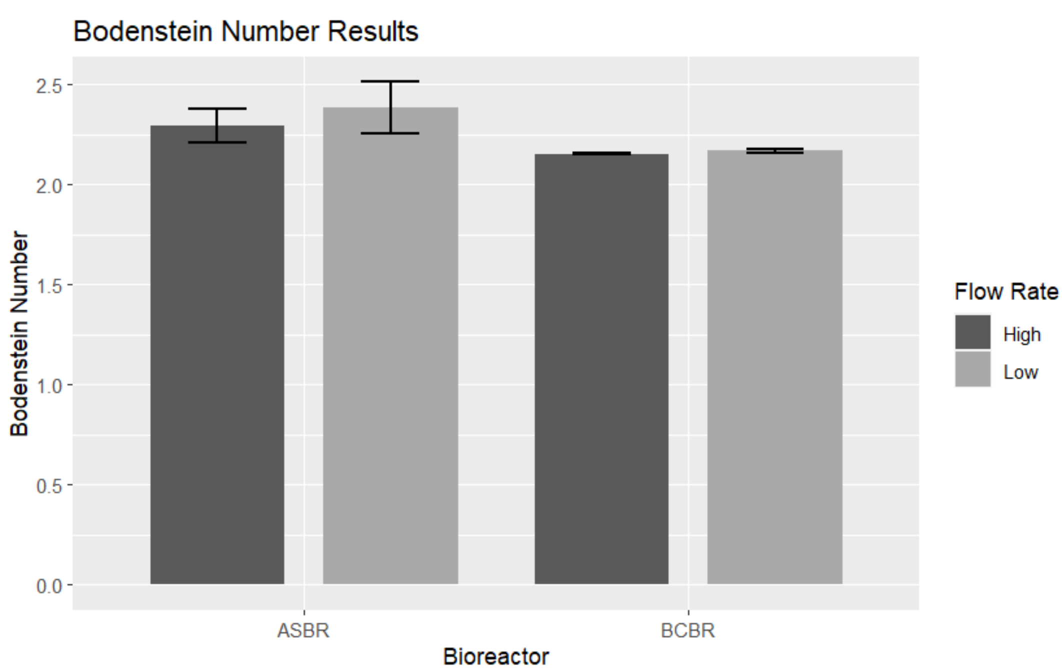

Figure 19. Depicts the mean and standard deviation for each treatment group for the Bodenstein Number results.

The t-test results show that there was a statistically significant difference in the average residence time between the bioreactors at the low flow rate with a p-value of 0.023 but no significant difference for the high flow rate with a p-value of 0.197. There was no statistically significant difference in the Vessel Distribution number between the bioreactors with a p-value of 0.095 and 0.090 for the high and low flow rates respectively. There was also no statistically significant difference in the Bodenstein number between the bioreactors with a p-value of 0.101 and 0.102 for the high and low flow rates respectively. The values were greater for the BCBR signifying greater mixing as compared to the ASBR. Greater mixing is conducive to the algal growth rate, although this difference may be explained by the defined flow path of the ASBR.

2.3.4 Oxygen Liquid Mass Transfer Coefficient

The logarithmic transformation was applied to the dissolved oxygen data to determine the oxygen liquid mass transfer coefficient (K_La) as shown in Figure 20 for the ASBR and Figure 21 for the BCBR.

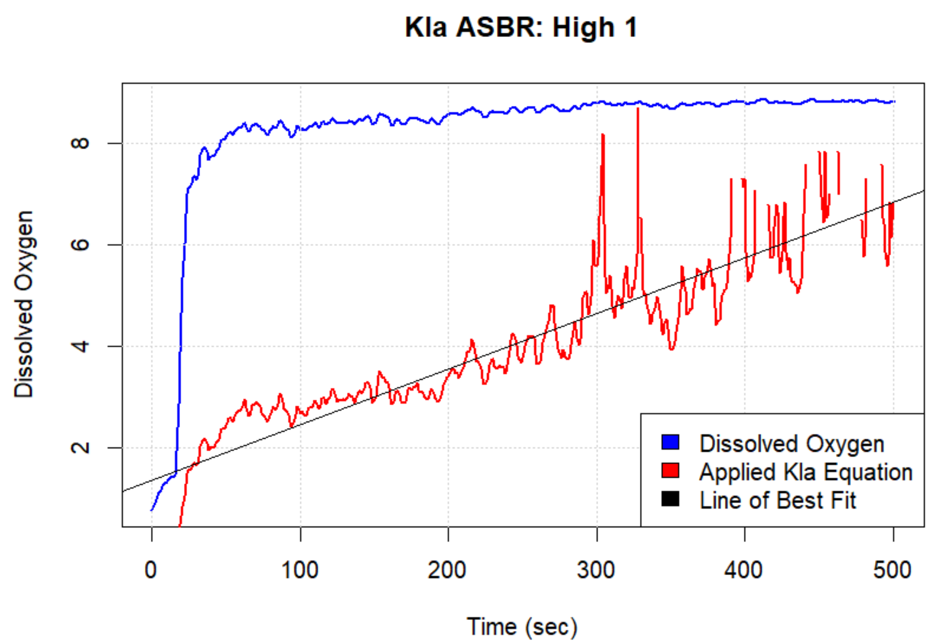

Figure 20. Kla transformation results for one of the replicates for the ASBR.

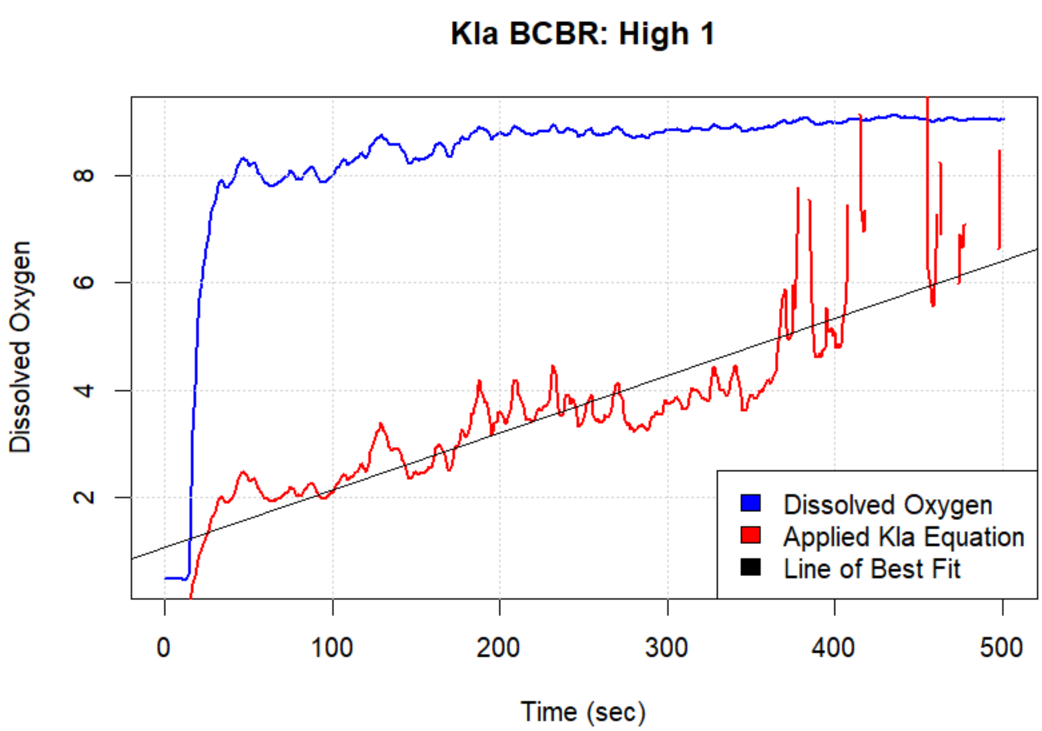

Figure 21. Kla transformation results for one of the replicates for the BCBR.

Each replication result is graphically shown in Figures 36 to 39 in the Appendix. Table 4 shows the values for each treatment and replication.

Table 4. Kla results for all treatment groups.

OXYGEN LIQUID MASS TRANSFER COEFFICIENT RESULTS (Units: 1/seconds)						
	Flow Rate	**Replicate 1**	**Replicate 2**	**Replicate 3**	**Mean**	**Std. Dev.**
ASBR	*High*	0.011	0.011	0.013	0.012	0.001
	Low	0.009	0.008	0.011	0.009	0.002
BCBR	*High*	0.011	0.010	0.011	0.011	0.001
	Low	0.001	0.001	0.005	0.002	0.003

The mean K_La and standard deviation for each treatment group are shown in Figure 22 below.

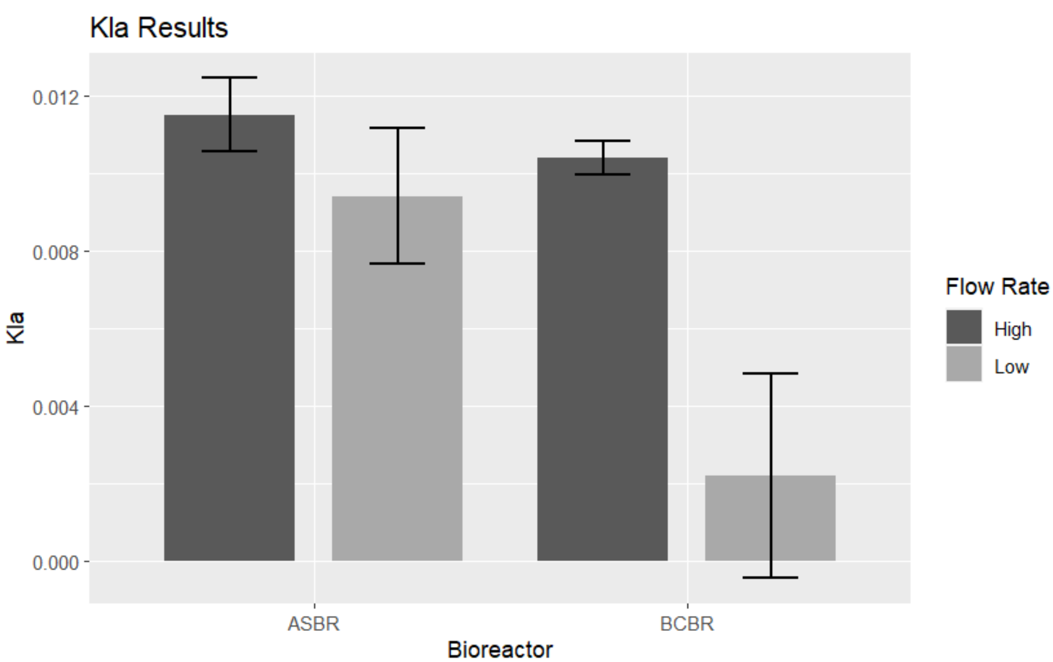

Figure 22. Depicts the mean and standard deviation for each treatment group for the Kla results.

The t-test result for the high flow rate showed no statistically significant difference between the bioreactors with a p-value of 0.173. Whereas the low flow rate resulted in a statistically significant difference with a p-value of 0.022. The mass transfer coefficient was significantly higher for the ASBR which signifies greater mass transfer and thus is conducive to a higher algal growth rate compared to the BCBR due to improved gas availability and distribution.

2.3.5 Sparger Arrangements

The three sparger arrangements were analyzed by measuring the mixing time; therefore, the moving average was applied to each replicate graph as shown in Section 2.3.1. Each replication result is graphically shown in Figures 26 to 31 in the Appendix. Table 5 shows the values for each treatment and replication.

Table 5. Mixing Time results for all six treatment groups.

MIXING TIME RESULTS: BCBR WITH 3 SPARGER ARRANGEMENTS (Units: sec.)						
	Flow Rate	**Replicate 1**	**Replicate 2**	**Replicate 3**	**Mean**	**Std. Dev.**
Arrangement	*High*	28.9	23.2	23.3	25.1	3.26
	Low	40.6	36.7	38.7	38.7	1.98
Arrangement	*High*	23.0	28.8	23.1	25.0	3.30
	Low	23.6	30.0	35.9	29.8	6.18
Arrangement 3	*High*	32.3	26.9	29.4	29.5	2.68
	Low	43.5	37.9	36.2	39.2	3.78

The mean mixing time and standard deviation for each treatment group are shown in Figure 23 below.

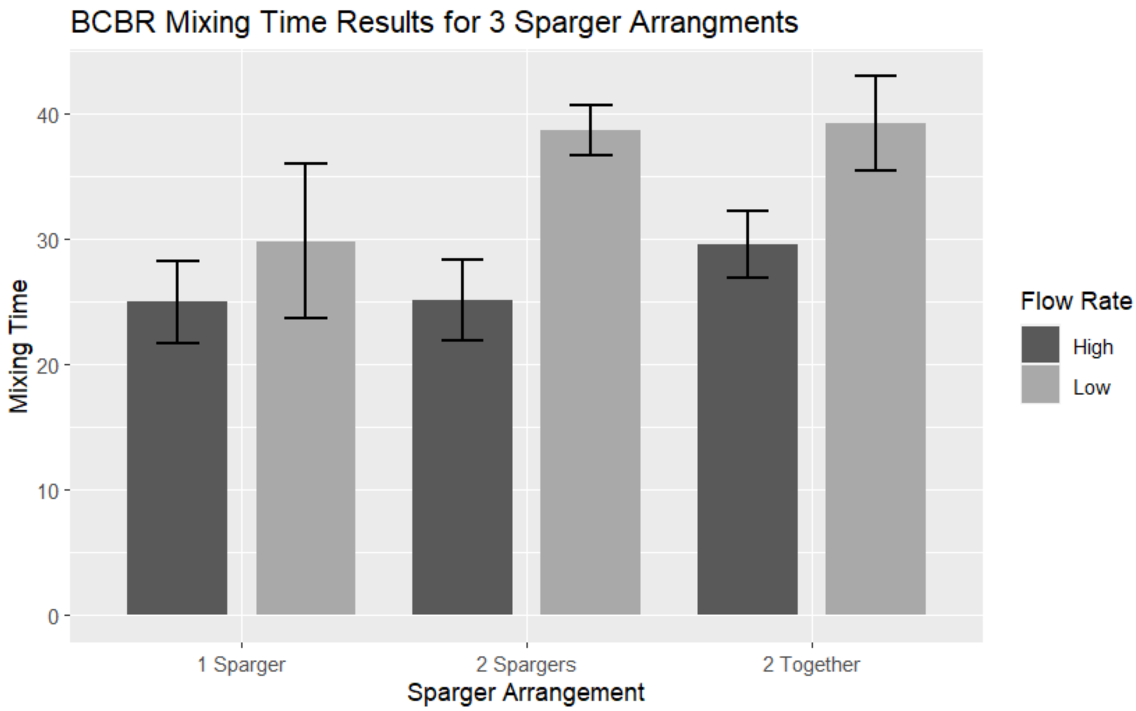

Figure 23. Depicts the mean and standard deviation for each sparger arrangement and flow rate for the Mixing Time results in the BCBR.

The ANOVA test results showed no significant differences in the mixing time results for all 3 sparger arrangements and both flow rates. The p-values for the high and low flow rate mixing time results are 0.200 and 0.066 respectively, both greater than the significance level of 0.05. This signifies that there was not a significant impact on the mixing time results based on the location and number of spargers that were tested in the BCBR.

2.4 Conclusion

The principal conclusions drawn from the results were as follows: (1) the BCBR exhibits greater liquid mixing compared to the ASBR, a desired factor for algal growth rate; (2) the ASBR demonstrates greater mass transfer than the BCBR, also a desired factor for algal growth rate; and (3) the placement and amount of spargers did not affect the mixing time results in the BCBR.

The faster mixing time observed in the BCBR can be explained by the flow path in the BCBR versus the ASBR. Due to the ASBR having a defined flow path, its bulk liquid mixing is constrained to take place within the relatively narrow confines of such a flow path wherein the collision impact of liquid elements is restricted within the flow path. By contrast, with the BCBR having no defined flow path, its bulk liquid mixing is achieved more efficiently through the freer and unconstrained movement throughout the bulk volume of the fluid elements as they collide, thereby enabling a more efficient propagation of the collision impact resulting in faster mixing of the fluid elements. Therefore, it was expected that our results associated with mixing will be longer in the ASBR when compared to the BCBR. While a short mixing time is desired, a defined flow path resulting in higher mixing times might still facilitate better mass transfer and light distribution. Additionally, in terms of large-scale implementation, it is important to have a defined flow path. Without a defined path, there may be a large amount of variability in the BCBR if implemented at a commercial scale. Predictability and replicability are important in commercial applications in order for microalgae production to be consistent and reliable. The ASBR's unique air lift design ensures a constant flow regime regardless of the size of the system. The longer Residence Time in the BCBR is attributed to the movement of particles. As the BCBR does not have a defined flow path, the particles are distributed more randomly. Therefore, the tracer molecule is going to take longer to leave the bioreactor thus leading to a longer residence time.

The oxygen liquid mass transfer results demonstrate a significant improvement in the ASBR as opposed to the BCBR as Kla is a key component in the success of algal growth. It is necessary for there to be adequate gas transfer in terms of oxygen leaving the system and carbon dioxide entering in order for the algal cells to undergo photosynthesis and grow in ideal conditions. This proves that even though the ASBR had a less desirable mixing result, it still resulted in a greater mass transfer which is directly related to the algal growth rate. Lastly, we concluded that the placement and amount of spargers did not affect our mixing time results in the BCBR, as it showed no significant differences. This could potentially lead to energy savings in terms of aeration. Based on the residence time and KLa results, as well as the expected replicability and reliability of the hydrodynamics on scale-up, it is anticipated that the ASBR will outperform the BCBR significantly. Therefore, it is worth exploring the ASBR, even though it may come with a higher economic burden.

Future experiments should be conducted to investigate the algal growth rate to further support these findings. Residence Time Distribution experiments could ideally be conducted with a designated output, rather than using a siphon, and more data could be collected to limit the effect of the extrapolation. Additionally, a more comprehensive analysis could be conducted solely on the RTD, in which the flow patterns are modeled in more depth, such as using Computational Fluid Dynamics (CFD). Lastly, the ASBR can be implemented at pilot-scale to examine the consistency of the hydrodynamics as the system size is increased and further prepare the ASBR for commercial-scale applications.

APPENDIX

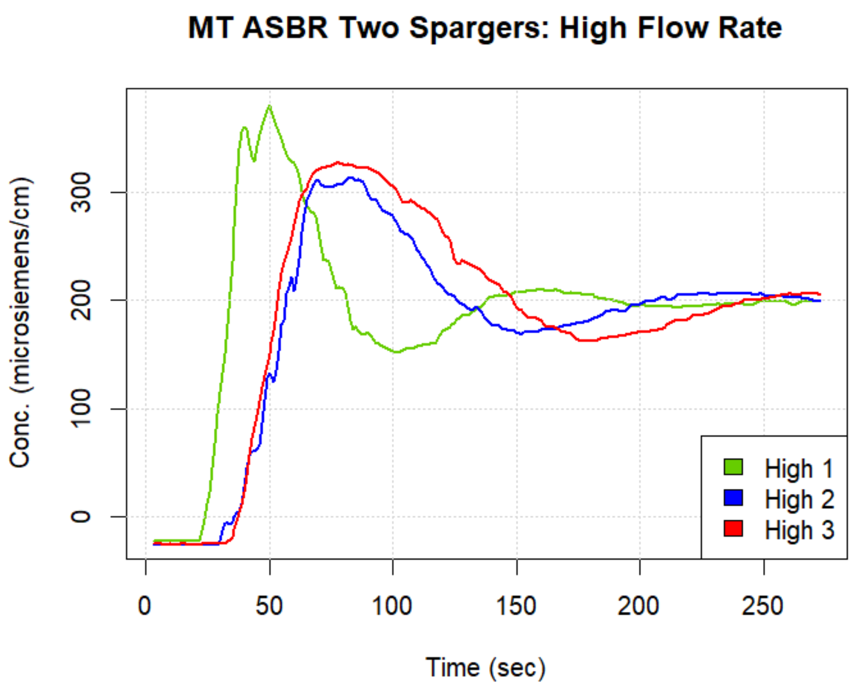

Figure 24. Mixing Time results for each replicate for the high flow rate for the ASBR.

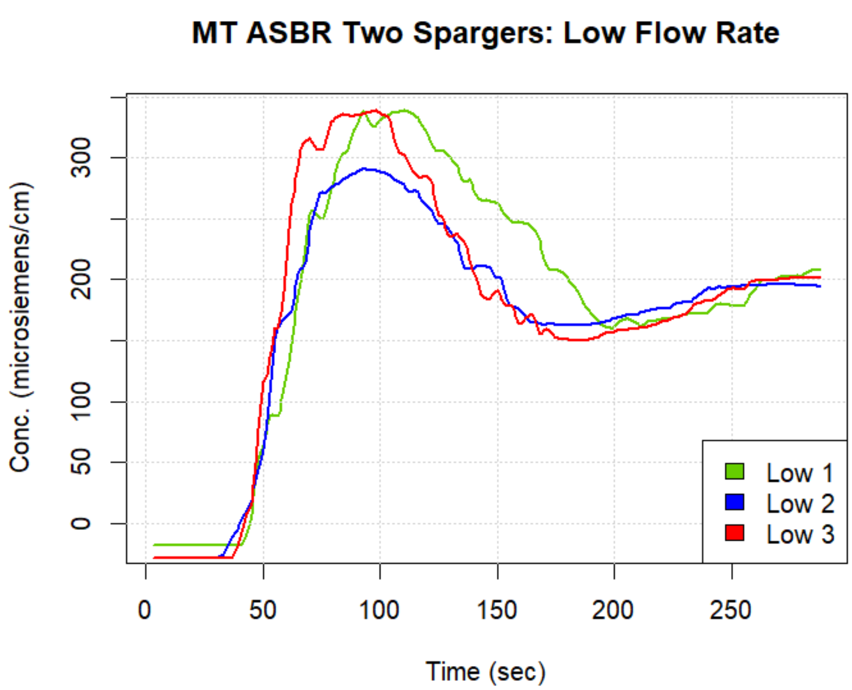

Figure 25. Mixing Time results for each replicate for the low flow rate for the ASBR.

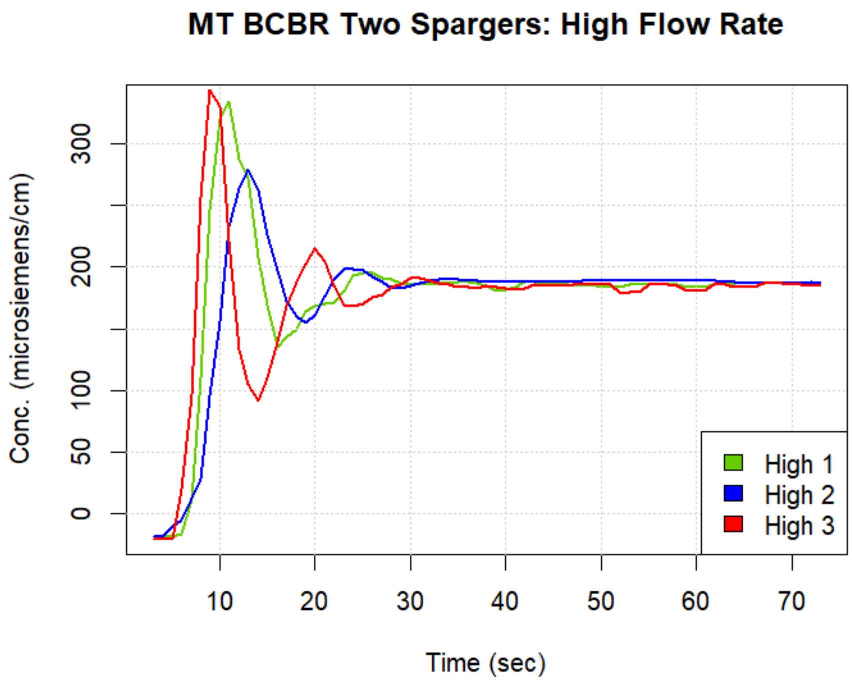

Figure 26. Mixing Time results for each replicate for the high flow rate for the BCBR.

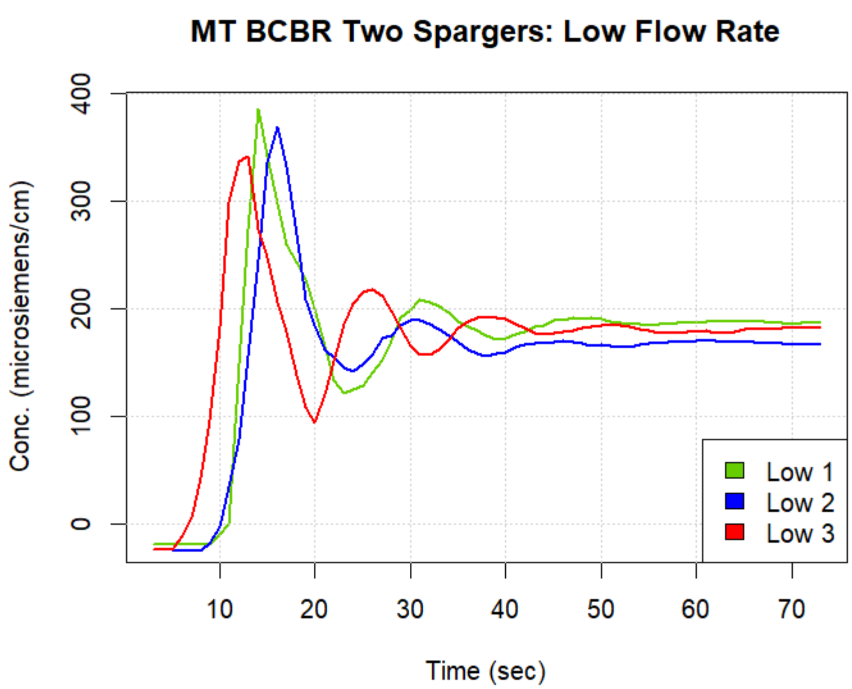

Figure 27. Mixing Time results for each replicate for the low flow rate for the BCBR.

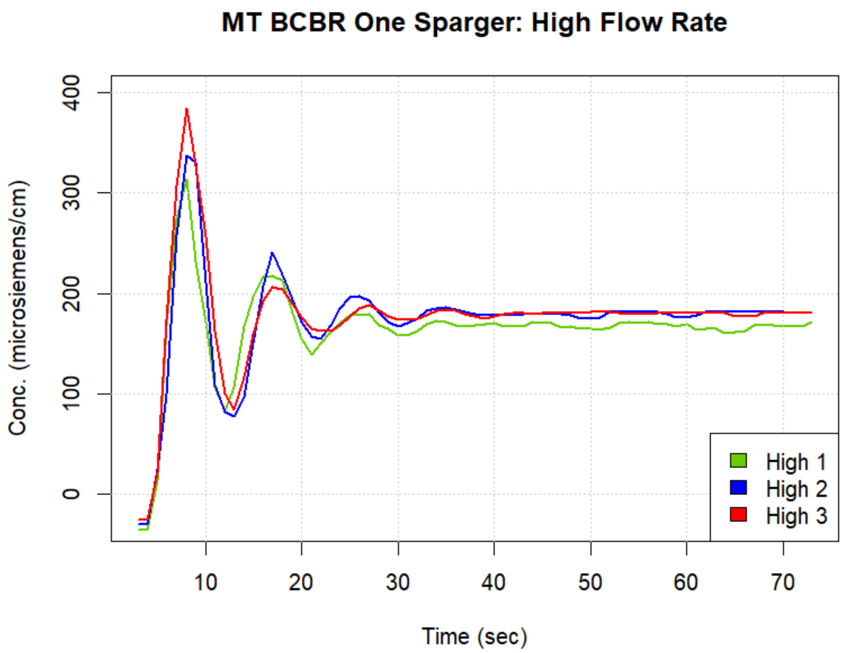

Figure 28. Mixing Time results for each replicate for the single sparger arrangement for the high flow rate for the BCBR.

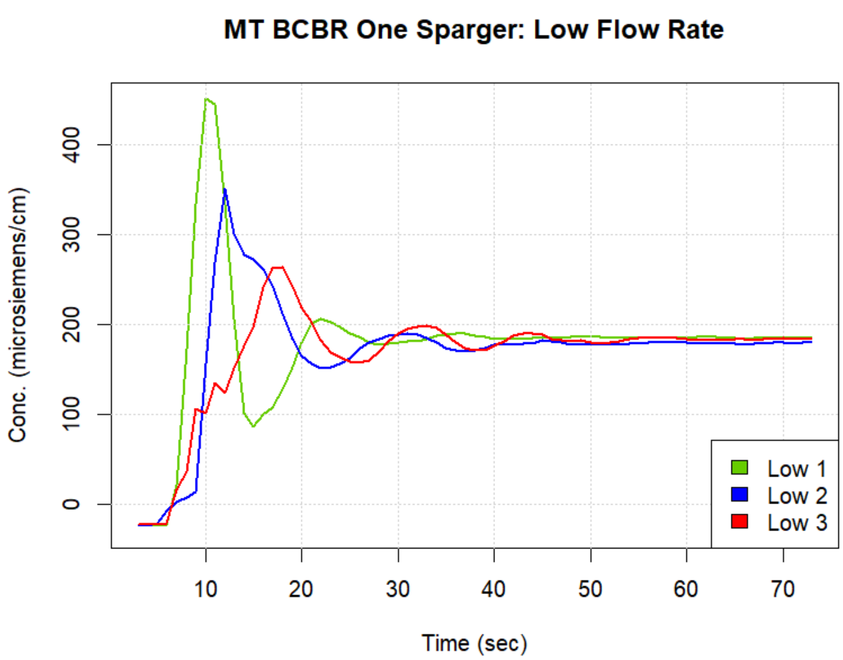

Figure 29. Mixing Time results for each replicate for the single sparger arrangement for the low flow rate for the BCBR.

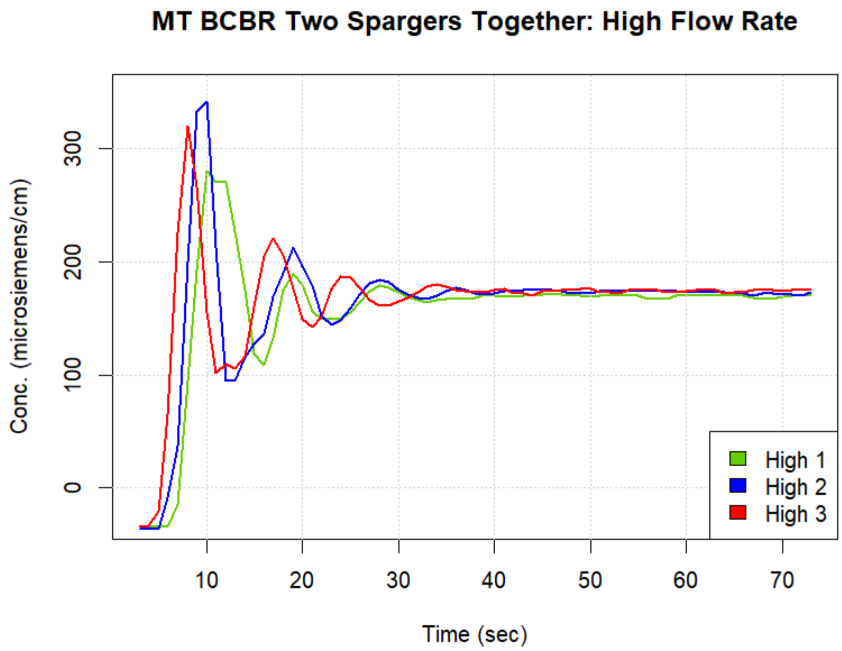

Figure 30. Mixing Time results for each replicate for the sparger arrangement in which two spargers are placed together for the high flow rate for the BCBR.

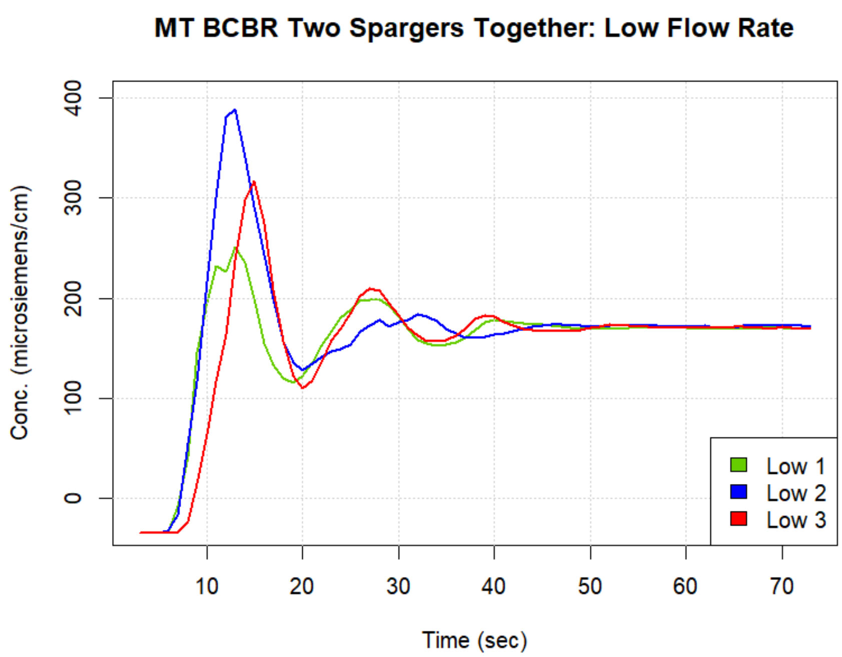

Figure 31. Mixing Time results for each replicate for the sparger arrangement in which two spargers are placed together for the low flow rate for the BCBR.

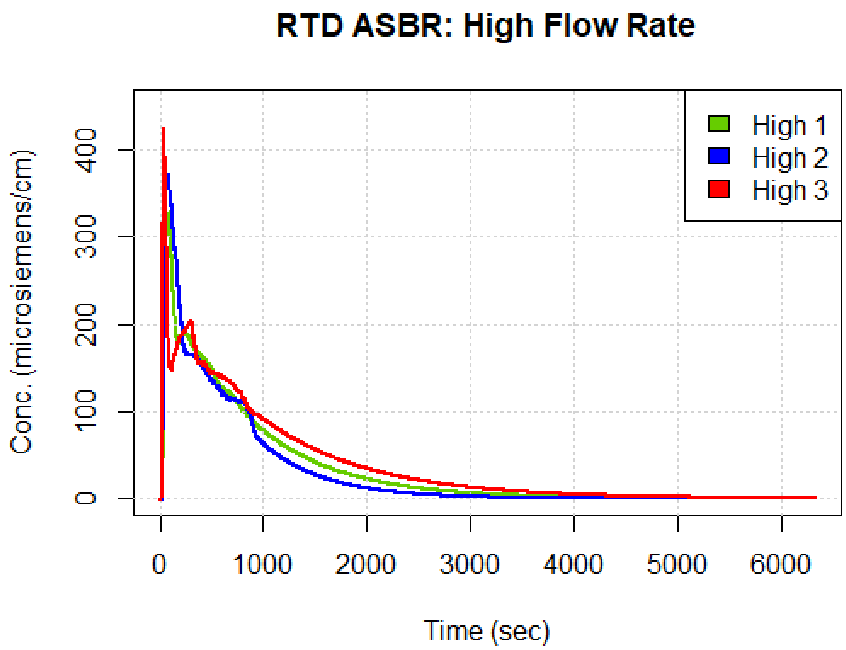

Figure 32. Residence Time results for each replicate for the high flow rate for the ASBR.

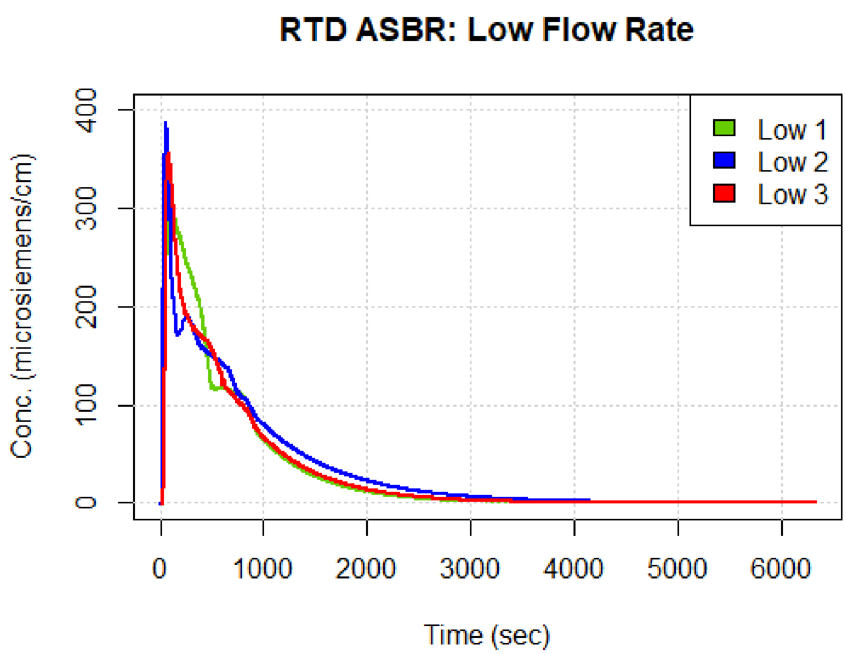

Figure 33. Residence Time results for each replicate for the low flow rate for the ASBR.

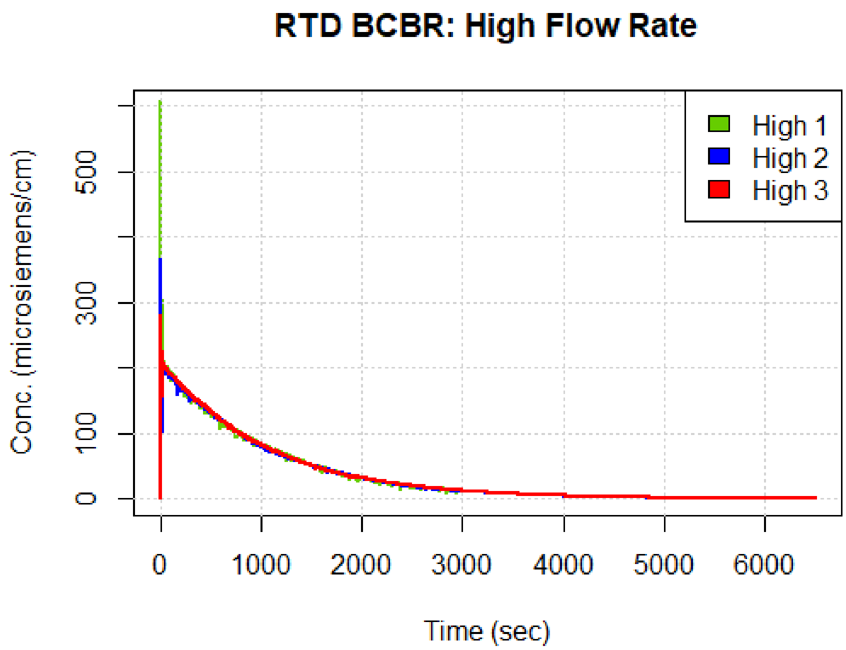

Figure 34. Residence Time results for each replicate for the high flow rate for the BCBR.

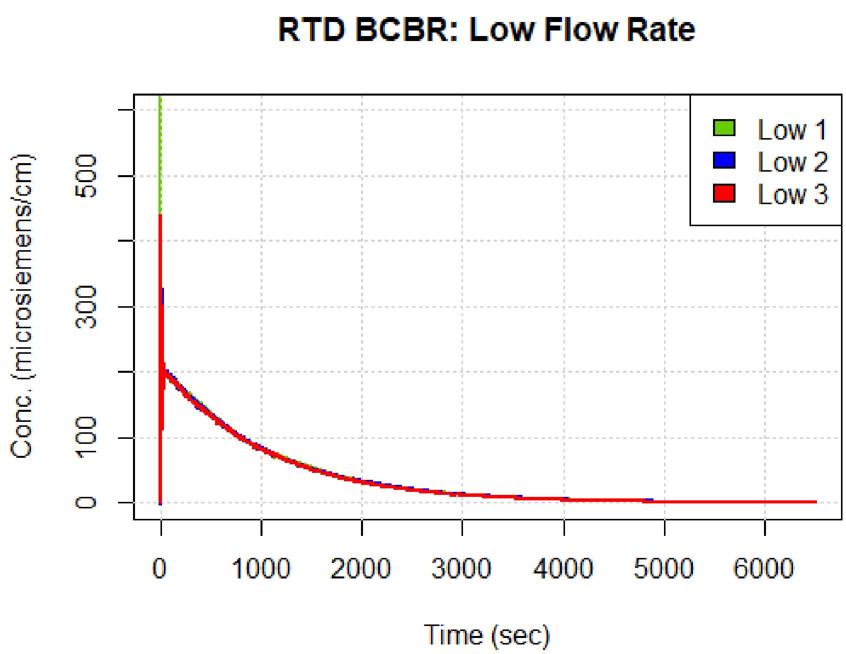

Figure 35. Residence Time results for each replicate for the low flow rate for the BCBR.

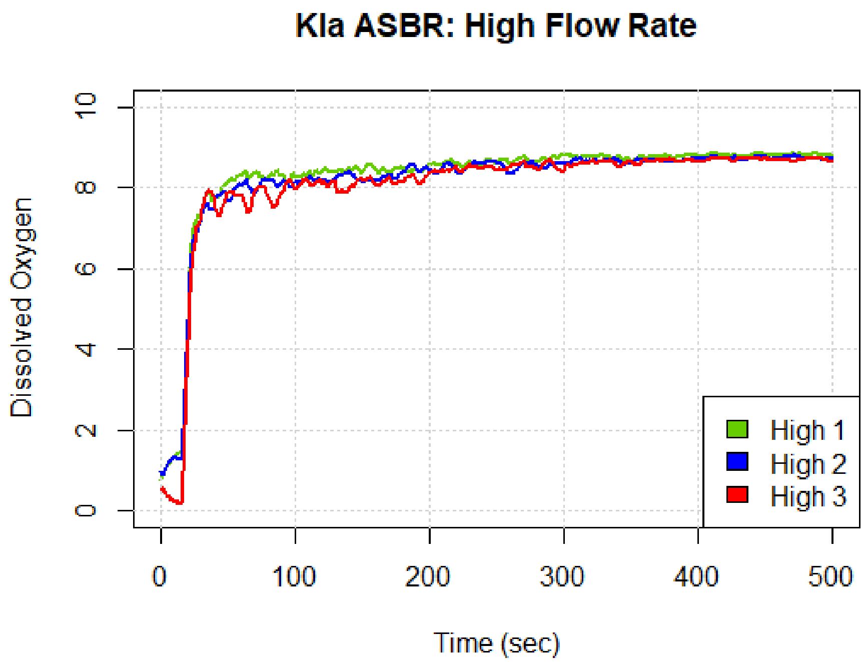

Figure 36. KLa results for each replicate for the high flow rate for the ASBR.

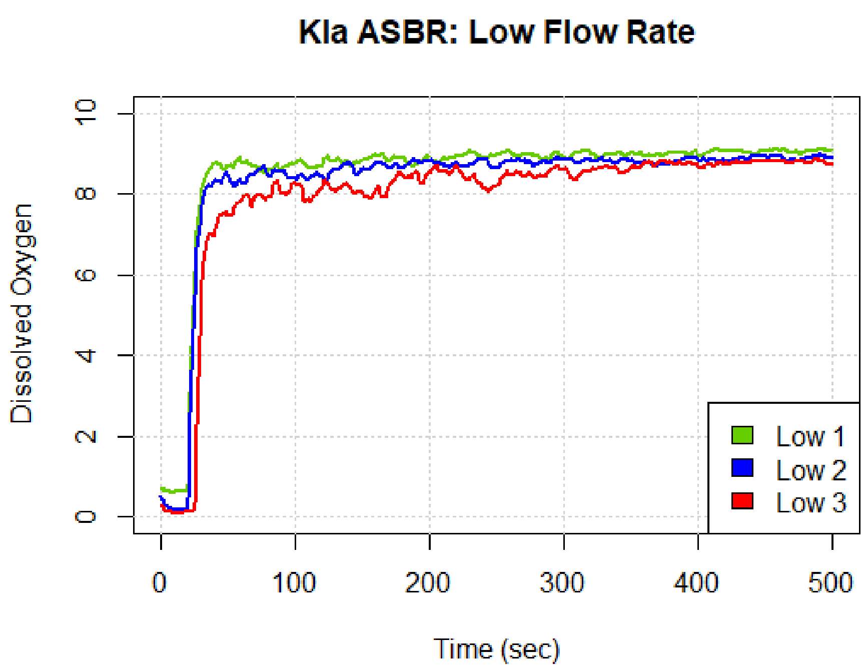

Figure 37. KLa results for each replicate for the low flow rate for the ASBR.

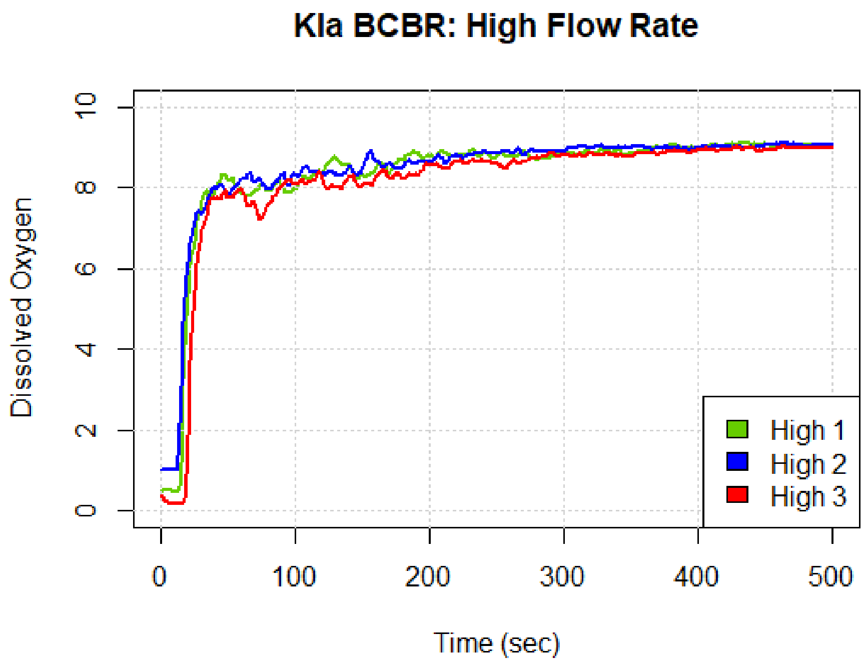

Figure 38. KLa results for each replicate for the high flow rate for the BCBR.

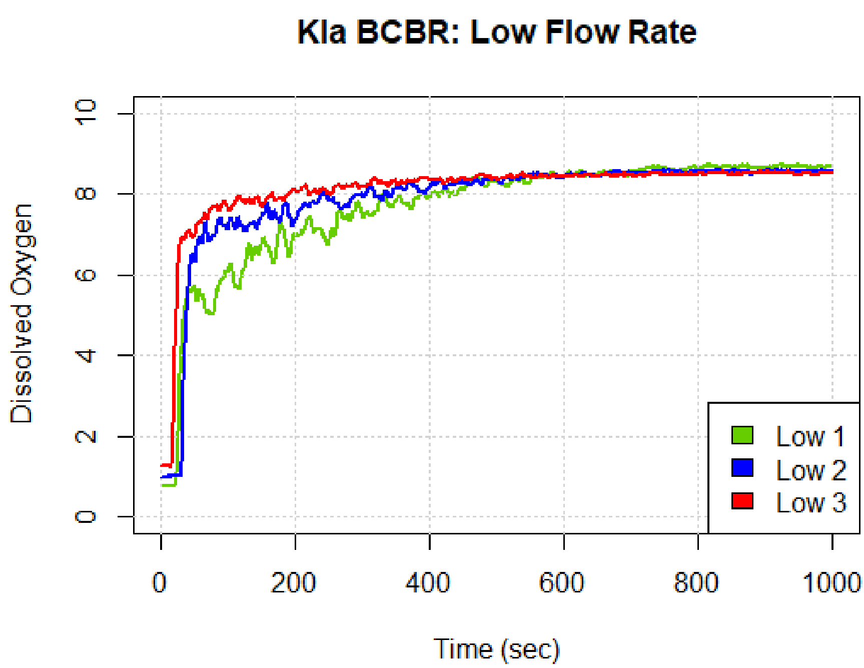

Figure 39. KLa results for each replicate for the low flow rate for the BCBR.

Code 1. Mixing Time

```
#MT code for ASBR with two spargers
#with 3 second moving average filter

library(openxlsx)

# specifying data to be read in
filename <- 'C:/Users/hailey/OneDrive/Documents/MTData_ASBR2.xlsx'
sheets <- c('High 1', 'High 2', 'High 3', 'Low 1', 'Low 2', 'Low 3')

# reading in the data
for (idx in 1:length(sheets)) {
  data <- read.xlsx(filename, sheet = sheets[idx], startRow = 13,
colNames = FALSE)
  if (idx %in% c(1, 2, 3)) {
    # specifying columns to be read in and converted to numeric
    numeric_columns <- c(3, 4)
    data[, numeric_columns] <- apply(data[, numeric_columns, drop =
FALSE], 2, as.numeric)

    inject_time <- as.numeric(data[1:275, 3])
    C <- data[1:275, 4]
  } else {
    # specifying columns to be read in and converted to numeric
    numeric_columns <- c(3, 4)
    data[, numeric_columns] <- apply(data[, numeric_columns, drop =
FALSE], 2, as.numeric)

    inject_time <- as.numeric(data[1:290, 3])
    C <- data[1:290, 4]
  }
  # Calculate moving average
  filt_time <- 3
  new_data <- numeric(length(C) - filt_time - 1)
  new_time <- numeric(length(C) - filt_time - 1)

  for (ind in 1:(length(C) - filt_time - 1)) {
    new_data[ind] <- mean(C[ind:(ind + filt_time - 1)])
    new_time[ind] <- inject_time[ind + filt_time - 1]
  }


  # Calculate mean and +- 5% values
  avg <- mean(tail(new_data, 25))
  plus5 <- ceiling(avg * 1.05)
  minus5 <- floor(avg * 0.95)

  # Linear interpolation
  range <- c(minus5, plus5)
```

```
  # Find values out of range
  outRange <- which(new_data <= range[1] | new_data >= range[2])
  MT <- max(outRange)

  # Plot graph
  plot(inject_time, C, type = 'l', lwd = 2, col = 'purple',
       xlab = 'Time (sec)', ylab = 'Conc. (microsiemens/cm)',
       main = paste('MT ASBR Two Spargers:', sheets[idx]))
  grid()
  lines(new_time, new_data, type = 'l', lwd = 2, col = 'blue')
  abline(h = plus5, col = 'red', lty = 2, lwd = 2)   # line for plus5
  abline(h = minus5, col = 'green', lty = 2, lwd = 2) # line for
minus5
  points(new_time[MT], new_data[MT], pch = 16, cex = 1.5, col =
'black') # point for MT
  legend(x="bottomright", legend = c("Raw Data", "Filtered Data",
"Plus 5%", "Minus 5%", "Mixing Time"), fill = c("purple", "blue",
"red", "green", "black"))

  # determine exact MT using linear interpolation
  plus5exact <- avg * 1.05
  minus5exact <- avg * 0.95

  # range for MT determination
  rangeexact <- c(minus5exact, plus5exact)

  # Find values out of range
  outRangeexact <- which(new_data <= rangeexact[1] | new_data >=
rangeexact[2])
  MTexact <- max(outRangeexact)
  tIntersect = (((new_data[MTexact] - new_data[MTexact-
2])*(new_time[MTexact+2] - new_time[MTexact-2]))/(new_data[MTexact+2]
- new_data[MTexact-2])) + new_time[MTexact-2]
  print(tIntersect)

  #create lists for each sheet of data
  if (idx ==1) {
    high1 <- new_data
  } else if (idx ==2) {
    high2 <- new_data
  } else if (idx == 3) {
    high3 <- new_data
  } else if (idx == 4) {
    low1 <- new_data
  } else if (idx == 5) {
    low2 <- new_data
  } else {
    low3 <- new_data
  }

}
```

```
#create new time to match length of high flow rate data
high_time <- new_time[1:271]

#plotting high flow rate data
plot(high_time, high1, type = 'l', lwd = 2, col = 'chartreuse3',
    xlab = 'Time (sec)', ylab = 'Conc. (microsiemens/cm)',
    main = paste('MT ASBR Two Spargers: High Flow Rate'))
grid()
lines(high_time, high2, type = 'l', lwd = 2, col = 'blue')
lines(high_time, high3, type = 'l', lwd = 2, col = 'red')
legend(x="bottomright", legend = c("High 1", "High 2", "High 3"), fill
= c("chartreuse3", "blue", "red"))

#plotting low flow rate data
plot(new_time, low1, type = 'l', lwd = 2, col = 'chartreuse3',
    xlab = 'Time (sec)', ylab = 'Conc. (microsiemens/cm)',
    main = paste('MT ASBR Two Spargers: Low Flow Rate'))
grid()
lines(new_time, low2, type = 'l', lwd = 2, col = 'blue')
lines(new_time, low3, type = 'l', lwd = 2, col = 'red')
legend(x="bottomright", legend = c("Low 1", "Low 2", "Low 3"), fill =
c("chartreuse3", "blue", "red"))
```

Code 2. Residence Time Distribution

```
#RTD CODE FOR ASBR
#INCLUDES EXTRAPOLATION
#OFFSETS BIAS
#NORMALIZES CURVE

#install.packages("openxlsx")
#install.packages("minpack.lm")
library(openxlsx)
library(minpack.lm)

filename <- 'C:\\Users\\haile\\OneDrive\\Documents\\RTDdata_ASBR.xlsx'
sheets <- c('Low 1', 'Low 2', 'Low 3', 'High 1', 'High 2', 'High 3')

for (idx in 1:length(sheets)) {
  if (idx == 5) {
    data <- read.xlsx(filename, sheet = sheets[idx], startRow = 67,
colNames = FALSE)
    inject_time <- as.numeric(data[1:936, 3])
    C <- as.numeric(data[1:936, 4]) - as.numeric(data[1,4])
  } else {
    data <- read.xlsx(filename, sheet = sheets[idx], startRow = 63,
colNames = FALSE)
    inject_time <- as.numeric(data[1:940, 3])
    C <- as.numeric(data[1:940, 4]) - as.numeric(data[1,4])
```

```
  }



  # Extrapolate
  maxT <- which.max(C)
  new_time <- inject_time[maxT:length(inject_time)]
  new_C <- C[maxT:length(C)]

  expDecay <- function(x, a, b) {
    a * exp(b*x)
  }

  fit <- nlsLM(new_C ~ expDecay(new_time, a, b), start = list(a = 213,
b = -0.001))

  time_fit <- seq(0,6330, by = 1)

  predictedC <- predict(fit, newdata = data.frame(new_time =
time_fit))

  #bleed
  dataEnd <- max(length(C))
  dataEnd
  extrapEnd <- 6330
  time <- c(1:6330)
  num <- 100

  diffBleed <- -(C[dataEnd]-predictedC[dataEnd])

  jump <- c(0:num)

  for (index in 2:num) {
    jump[index] <- jump[index-1]+diffBleed/num
  }

  combinedC <- c(C[0:(dataEnd-num)], (C[(dataEnd-(num-
1)):dataEnd]+jump[1:num]) , predictedC[(dataEnd + 1):6330])



  # Plot concentrate
  plot(inject_time, C, type = 'l', lwd = 2, col = 'blue', xlab = 'Time
(sec)', ylab = 'Conc. (microsiemens/cm)', main = paste('RTD ASBR',
sheets[idx]), xlim = c(min(inject_time), max(time_fit)))
  grid()
  lines(time_fit, predictedC, col = 'red')
  lines(time, combinedC, lwd = 1.5, col = 'black')
  legend(x="topright", legend = c("Collected Data", "Exponential Decay
Extrapolation", "Combined Data"), fill = c("blue", "red", "black"))

  # Calculating average residence time
```

```
  Cxt <- combinedC * time
  sumnum <- sum(Cxt)
  sumdenom <- sum(combinedC)
  avgRes <- sumnum / sumdenom
  print(avgRes)

  # Calculating vessel dispersion number
  Cxt2 <- combinedC * time * time
  sum2 <- sum(Cxt2)
  sigma2 <- (sum2/sumdenom)-((sumnum/sumdenom)^2)
  sigman2 <- sigma2/avgRes^2
  vesselDisp <- sigman2/2
  print(vesselDisp)

  #Calculating Bodenstein number
  bodenstein <- 1/vesselDisp
  print(bodenstein)

  # Calculate area and RTD
  deltas <- sum(diff(combinedC))
  area <- deltas * time[length(time)]
  RTD <- combinedC / area

  # Plot RTD
  plot(time, RTD, type = 'l', lwd = 2, col = 'green', xlab = 'Time
(sec)', ylab = 'RTD', main = paste('RTD ASBR', sheets[idx]))
  grid()

  # Check
  area_RTD <- sum(diff(RTD)) * time[length(time)]
  print(area_RTD)

  #create lists for each sheet of data
  if (idx ==1) {
    low1 <- combinedC
  } else if (idx ==2) {
    low2 <- combinedC
  } else if (idx == 3) {
    low3 <- combinedC
  } else if (idx == 4) {
    high1 <- combinedC
  } else if (idx == 5) {
    high2 <- combinedC
  } else {
    high3 <- combinedC
  }

}


#plotting high flow rate data
plot(time, high1, type = 'l', lwd = 2, col = 'chartreuse3',
```

```
     xlab = 'Time (sec)', ylab = 'Conc. (microsiemens/cm)',
     main = paste('RTD ASBR: High Flow Rate'), ylim = c(0,450))
grid()
lines(time, high2, type = 'l', lwd = 2, col = 'blue')
lines(time, high3, type = 'l', lwd = 2, col = 'red')
legend(x="topright", legend = c("High 1", "High 2", "High 3"), fill =
c("chartreuse3", "blue", "red"))

#plotting low flow rate data
plot(time, low1, type = 'l', lwd = 2, col = 'chartreuse3',
     xlab = 'Time (sec)', ylab = 'Conc. (microsiemens/cm)',
     main = paste('RTD ASBR: Low Flow Rate'), ylim = c(0,400))
grid()
lines(time, low2, type = 'l', lwd = 2, col = 'blue')
lines(time, low3, type = 'l', lwd = 2, col = 'red')
legend(x="topright", legend = c("Low 1", "Low 2", "Low 3"), fill =
c("chartreuse3", "blue", "red"))
```

Code 3. Oxygen Liquid Mass Transfer Coefficient (K_La)

```
#Kla Code
#with logarithmic transformation
#line of best fit for logarithmic transformation
#slope of line of best fit is kla


library(openxlsx)


filename <- 'C:\\Users\\haile\\OneDrive\\Documents\\KLAData_ASBR.xlsx'
sheets <- c('Low 1', 'Low 2', 'Low 3', 'High 1', 'High 2', 'High 3')

for (idx in 1:length(sheets)) {
    data <- read.xlsx(filename, sheet = sheets[idx], startRow = 2,
colNames = FALSE)
    time <- as.numeric(data[1:502, 1])
    kla <- as.numeric(data[1:502, 2])

  klaData <- numeric(length(kla) - 1)
  klaTime <- time[1:(length(kla) - 1)]

  #applying kla equation

  for (ind in 1:(length(kla)-1)){

    klaData[ind] <- -log((kla[length(kla)]-kla[ind])/(kla[length(kla)]
- kla[1]))

  }
```

```
  #plot
  plot(time, kla, type = 'l', lwd = 2, col = 'blue',
       xlab = 'Time (sec)', ylab = 'Dissolved Oxygen',
       main = paste('Kla ASBR:', sheets[idx]))
  grid()
  lines(klaTime, klaData, type = 'l', lwd = 2, col = 'red')

  # Remove NA, NaN, Inf values from klaData
  clean_indices <- is.finite(klaData)
  klaData_clean <- klaData[clean_indices]
  klaTime_clean <- klaTime[clean_indices]

  # Add line of best fit
  abline(lm(klaData_clean ~ klaTime_clean), col = 'black')
  legend(x="bottomright", legend = c("Dissolved Oxygen", "Applied Kla
Equation", "Line of Best Fit"), fill = c("blue", "red", "black"))
  coeffs <- summary(lm(klaData_clean ~ klaTime_clean))
  print(coeffs)

  #create lists for each sheet of data
  if (idx ==1) {
    low1 <- kla
  } else if (idx ==2) {
    low2 <- kla
  } else if (idx == 3) {
    low3 <- kla
  } else if (idx == 4) {
    high1 <- kla
  } else if (idx == 5) {
    high2 <- kla
  } else {
    high3 <- kla
  }

}



#plotting high flow rate data
plot(time, high1, type = 'l', lwd = 2, col = 'chartreuse3',
     xlab = 'Time (sec)', ylab = 'Dissolved Oxygen',
     main = paste('Kla ASBR: High Flow Rate'), ylim = c(0,10))
grid()
lines(time, high2, type = 'l', lwd = 2, col = 'blue')
lines(time, high3, type = 'l', lwd = 2, col = 'red')
legend(x="bottomright", legend = c("High 1", "High 2", "High 3"), fill
= c("chartreuse3", "blue", "red"))

#plotting low flow rate data
plot(time, low1, type = 'l', lwd = 2, col = 'chartreuse3',
     xlab = 'Time (sec)', ylab = 'Dissolved Oxygen',
     main = paste('Kla ASBR: Low Flow Rate'), ylim = c(0,10))
```

```
grid()
lines(time, low2, type = 'l', lwd = 2, col = 'blue')
lines(time, low3, type = 'l', lwd = 2, col = 'red')
legend(x="bottomright", legend = c("Low 1", "Low 2", "Low 3"), fill =
c("chartreuse3", "blue", "red"))
```

Code 4. Bar Plots

```
#bar plots for all experiments

#bar plot 1
#MT with 2 Spargers

# Load ggplot2 library
library(ggplot2)

# Data
df <- data.frame(
  Bioreactor = c("ASBR", "ASBR", "BCBR", "BCBR"),
  Flow = c("High", "Low", "High", "Low"),
  Mt = c(198.11, 247.09, 25.12, 38.65)
)

# Standard deviation values
Stdev <- c(35.16, 12.34, 3.26, 1.98)

# Create bar plot
ggplot(df, aes(x = Bioreactor, y = Mt, fill = Flow)) +
  geom_bar(stat = "identity", position = position_dodge(width = 0.9),
width = 0.7) +
  geom_errorbar(aes(ymin = Mt - Stdev, ymax = Mt + Stdev),
               position = position_dodge(width = 0.9), width = 0.3,
size = 0.8) + # Adding error bars
  labs(x = "Bioreactor", y = "Mixing Time", title = "Mixing Time
Results with 2 Spargers") +
  scale_fill_manual(values = c("gray35", "darkgray"))


#bar plot 2
#MT with 1 Sparger

library(ggplot2)

# Data
df <- data.frame(
  Bioreactor = c("ASBR", "ASBR", "BCBR", "BCBR"),
  Flow = c("High", "Low", "High", "Low"),
  Mt = c(181.59, 254.76, 24.95, 29.82)
)
```

```
# Standard deviation values
Stdev <- c(7.88, 21.41, 3.30, 6.18)

# Create bar plot
ggplot(df, aes(x = Bioreactor, y = Mt, fill = Flow)) +
  geom_bar(stat = "identity", position = position_dodge(width = 0.9),
width = 0.7) +
  geom_errorbar(aes(ymin = Mt - Stdev, ymax = Mt + Stdev),
                position = position_dodge(width = 0.9), width = 0.3,
size = 0.8) + # Adding error bars
  labs(x = "Bioreactor", y = "Mixing Time", title = "Mixing Time
Results with 1 Sparger") +
  scale_fill_manual(values = c("gray35", "darkgray"))


#bar plot 3
#BCBR with all 3 Sparger Arrangements

library(ggplot2)

# Data
df <- data.frame(
  Sparg = c("1 Sparger", "1 Sparger", "2 Spargers", "2 Spargers", "2
Together", "2 Together"),
  Flow = c("High", "Low", "High", "Low", "High", "Low"),
  Mt = c(24.95, 29.82, 25.12, 38.65, 29.55, 39.19)
)

# Standard deviation values
Stdev <- c(3.30, 6.18, 3.26, 1.98, 2.68, 3.78)

# Create bar plot
ggplot(df, aes(x = Sparg, y = Mt, fill = Flow)) +
  geom_bar(stat = "identity", position = position_dodge(width = 0.9),
width = 0.7) +
  geom_errorbar(aes(ymin = Mt - Stdev, ymax = Mt + Stdev),
                position = position_dodge(width = 0.9), width = 0.3,
size = 0.7) + # Adding error bars
  labs(x = "Sparger Arrangement", y = "Mixing Time", title = "BCBR
Mixing Time Results for 3 Sparger Arrangments") +
  scale_fill_manual(values = c("gray35", "darkgray"))


#bar plot 4
#Kla Results

library(ggplot2)

# Data
df <- data.frame(
  Bioreactor = c("ASBR", "ASBR", "BCBR", "BCBR"),
  Flow = c("High", "Low", "High", "Low"),
```

```
  Kla = c(0.0115, 0.0094, 0.0104, 0.0022)
)

# Standard deviation values
Stdev <- c(0.00095, 0.00175, 0.00044, 0.00263)

# Create bar plot
ggplot(df, aes(x = Bioreactor, y = Kla, fill = Flow)) +
  geom_bar(stat = "identity", position = position_dodge(width = 0.9),
width = 0.7) +
  geom_errorbar(aes(ymin = Kla - Stdev, ymax = Kla + Stdev),
                position = position_dodge(width = 0.9), width = 0.3,
size = 0.8) + # Adding error bars
  labs(x = "Bioreactor", y = "Kla", title = "Kla Results") +
  scale_fill_manual(values = c("gray35", "darkgray"))


#bar plot 5
#Average Residence Time Results
library(ggplot2)

# Data
df <- data.frame(
  Bioreactor = c("ASBR", "ASBR", "BCBR", "BCBR"),
  Flow = c("High", "Low", "High", "Low"),
  Rt = c(828.54,698.21, 1047.47, 1052.74)
)

# Standard deviation values
Stdev <- c(199.20, 96.82, 3.62, 8.57)

# Create bar plot
ggplot(df, aes(x = Bioreactor, y = Rt, fill = Flow)) +
  geom_bar(stat = "identity", position = position_dodge(width = 0.9),
width = 0.7) +
  geom_errorbar(aes(ymin = Rt - Stdev, ymax = Rt + Stdev),
                position = position_dodge(width = 0.9), width = 0.3,
size = 0.8) + # Adding error bars
  labs(x = "Bioreactor", y = "Avg. Residence Time", title = "Average
Residence Time Results") +
  scale_fill_manual(values = c("gray35", "darkgray"))


#bar plot 6
#Vessel Dispersion Results
library(ggplot2)

# Data
df <- data.frame(
  Bioreactor = c("ASBR", "ASBR", "BCBR", "BCBR"),
  Flow = c("High", "Low", "High", "Low"),
  Vd = c(0.4366,0.4206, 0.4643, 0.4617)
```

```
)

# Standard deviation values
Stdev <- c(0.0161, 0.023, 0.0011, 0.002)

# Create bar plot
ggplot(df, aes(x = Bioreactor, y = Vd, fill = Flow)) +
  geom_bar(stat = "identity", position = position_dodge(width = 0.9),
width = 0.7) +
  geom_errorbar(aes(ymin = Vd - Stdev, ymax = Vd + Stdev),
              position = position_dodge(width = 0.9), width = 0.3,
size = 0.8) + # Adding error bars
  labs(x = "Bioreactor", y = "Vessel Dispersion Number", title =
"Vessel Dispersion Results") +
  scale_fill_manual(values = c("gray35", "darkgray"))


#bar plot 7
#Bodenstein Results
library(ggplot2)

# Data
df <- data.frame(
  Bioreactor = c("ASBR", "ASBR", "BCBR", "BCBR"),
  Flow = c("High", "Low", "High", "Low"),
  Bo = c(2.2925,2.3822,2.1525,2.1659)
)

# Standard deviation values
Stdev <- c(0.0831,0.13,0.0048,0.0093)

# Create bar plot
ggplot(df, aes(x = Bioreactor, y = Bo, fill = Flow)) +
  geom_bar(stat = "identity", position = position_dodge(width = 0.9),
width = 0.7) +
  geom_errorbar(aes(ymin = Bo - Stdev, ymax = Bo + Stdev),
              position = position_dodge(width = 0.9), width = 0.3,
size = 0.8) + # Adding error bars
  labs(x = "Bioreactor", y = "Bodenstein Number", title = "Bodenstein
Number Results") +
  scale_fill_manual(values = c("gray35", "darkgray"))
```

Code 5. Statistical Analysis

```
#t tests to determine significant differences

#MT
#comparing high flow rate for MT with 2 spargers
MThighASBR <- c(165.75, 193.07, 235.52)
MThighBCBR <- c(28.88, 23.23, 23.25)
```

```
tTestMThigh <- t.test(MThighASBR, MThighBCBR)
tTestMThigh
#comparing low flow rate for MT with 2 spargers
MTlowASBR <- c(259.47, 234.79, 247.02)
MTlowBCBR <- c(40.62, 36.66, 38.66)
tTestMTlow <- t.test(MTlowASBR, MTlowBCBR)
tTestMTlow

#ANOVA
#comparing high flow rate for MT sparger arrangements
MThigh1 <- c(28.88, 23.23, 23.25)
MThigh2 <- c(22.98, 28.76, 23.11)
MThigh3 <- c(32.28, 26.93, 29.43)
data <- data.frame(
  values = c(MThigh1, MThigh2, MThigh3),
  group = factor(rep(1:3, each = 3))
)
anova_result <- aov(values ~ group, data = data)
print(summary(anova_result))
#comparing low flow rate for MT sparger arrangements
MTlow1 <- c(40.62, 36.66,38.66)
MTlow2 <- c(23.57, 29.97, 35.93)
MTlow3 <- c(43.45, 37.89, 36.24)
data <- data.frame(
  values = c(MTlow1, MTlow2, MTlow3),
  group = factor(rep(1:3, each = 3))
)
anova_result <- aov(values ~ group, data = data)
print(summary(anova_result))


#RTD
#comparing high flow rate for RT
RThighASBR <- c(827.11,630.05,1028.45)
RThighBCBR <- c(1043.62,1048.01,1050.79)
tTestRThigh <- t.test(RThighASBR, RThighBCBR)
tTestRThigh
#comparing low flow rate for RT
RTlowASBR <- c(620.68, 806.73, 667.21)
RTlowBCBR <- c(1054.81, 1060.09, 1043.33)
tTestRTlow <- t.test(RTlowASBR, RTlowBCBR)
tTestRTlow
#comparing high flow rate for Vessel Dist.
VdhighASBR <- c(0.4317, 0.4235, 0.4545)
VdhighBCBR <- c(0.4653,0.4645,0.4632)
tTestVdhigh <- t.test(VdhighASBR, VdhighBCBR)
tTestVdhigh
#comparing low flow rate for Vessel Dist.
VdlowASBR <- c(0.3984,0.4444,0.4191)
VdlowBCBR <- c(0.4640,0.4607,0.4604)
tTestVdlow <- t.test(VdlowASBR, VdlowBCBR)
tTestVdlow
```

```
#comparing high flow rate for Bodenstein
BohighASBR <- c(2.3164, 2.3610, 2.2000)
BohighBCBR <- c(2.1491, 2.1528, 2.1587)
tTestBohigh <- t.test(BohighASBR, BohighBCBR)
tTestBohigh
#comparing low flow rate for Bodenstein
BolowASBR <- c(2.5102, 2.2502, 2.3863)
BolowBCBR <- c(2.1552, 2.1705, 2.1720)
tTestBolow <- t.test(BolowASBR, BolowBCBR)
tTestBolow


#KLA
#comparing high flow rate for Bodenstein
KlahighASBR <- c(0.0110, 0.0109, 0.0126)
KlahighBCBR <- c(0.0106, 0.0099, 0.0107)
tTestKlahigh <- t.test(KlahighASBR, KlahighBCBR)
tTestKlahigh
#comparing low flow rate for Bodenstein
KlalowASBR <- c(0.0089, 0.0079, 0.0113)
KlalowBCBR <- c(0.0007, 0.0006, 0.0052)
tTestKlalow <- t.test(KlalowASBR, KlalowBCBR)
tTestKlalow
```

REFERENCES

Babcock, R. W., Malda, J., & Radway, J. C. (2002, January 11). *Hydrodynamics and mass transfer in a tubular airlift photobioreactor*. Springer Link. http://dx.doi.org/10.1023/A:1019924226457

Borowitzka, M. A. (2013, January 29). *High-value products from microalgae - their development and commercialisation*. Springer Link. https://doi.org/10.1007/s10811-013-9983-9

Chapman, R. L. (2010, September 1). *Algae: The world's most important "plants" - an introduction*. Springer Link. https://doi.org/10.1007/s11027-010-9255-9

Garrido-Cardenas, J. A., Manzano-Agugliaro, F., Acien-Fernandez, F. G., & Molina-Grima, E. (2018, August 23). *Microalgae Research Worldwide*. Algal Research. https://doi.org/10.1016/j.algal.2018.08.005

Leong, Y. K., Chang, J.-S., & Lee, D.-J. (2023, January 27). *Types of photobioreactors*. Elsevier. https://doi.org/10.1016/B978-0-323-99911-3.00007-5

Thoré, E. S. J., Muylaert, K., Bertram, M. G., & Brodin, T. (2023, February 6). *Microalgae*. Current Biology. https://doi.org/10.1016/j.cub.2022.12.032

Zuccaro, G., Yousuf, A., Pollio, A., & Steyer, J.-P. (2019, November 29). *Microalgae Cultivation Systems*. Science Direct. https://doi.org/10.1016/B978-0-12-817536-1.00002-3